Oligodendrocyte generation and maturation in the hippocampus may be a target of fluoxetine for delaying cognitive dysfunction during early Alzheimer's disease

Yi Zhang
Department of Laboratory Medicine, The Second Affiliated Hospital of Chongqing Medical University
Feng-lei Chao
Department of Histology and Embryology, Chongqing Medical University
Lei Zhang
Department of Histology and Embryology, Chongqing Medical University
Chun-ni Zhou
Department of Histology and Embryology, Chongqing Medical University
Lin Jiang
Experimental Teaching Management Center, Chongqing Medical University
Jing Tang
Department of Histology and Embryology, Chongqing Medical University
Xin Liang
Department of Histology and Embryology, Chongqing Medical University
Jin-hua Fan
Department of Histology and Embryology, Chongqing Medical University
Xiao-yun Dou
Academy of Life Sciences, Chongqing Medical University
Yong Tang (ytang062@163.com)
Chongqing Medical University https://orcid.org/0000-0002-8199-3985

Research

Keywords: Maturation, Oligodendrocytes, Hippocampus, Alzheimer's disease, Fluoxetine

Posted Date: February 26th, 2020

DOI: https://doi.org/10.21203/rs.2.24601/v1

Abstract

Background In the central nervous system, the myelin sheath and the cells that form it—oligodendrocytes—are associated with cognitive function. Oligodendrocyte abnormalities is an important early pathogenic factor of Alzheimer's disease (AD). However, it is unclear how the hippocampal oligodendrocytes change during early AD and whether early hippocampal oligodendrocyte pathology in AD can be regarded as a novel therapeutic target.

Methods To address these questions, we subjected APP/PS1 transgenic mice and nontransgenic littermates to fluoxetine interventions for 2 months. After intervention, the behaviors were assessed with open field test and Morris water maze test, the changes in hippocampal oligodendrocytes were studied using immunohistochemistry, immunofluorescence, unbiased stereological techniques, laser scanning confocal microscope and molecular biotechnology.

Results AD mice had an abnormally high number of oligodendrocyte lineage cells (Olig2 + cells) but lower expressions of CNPase and MBP and fewer mature oligodendrocytes (CNPase + cells) in the hippocampus than nontransgenic littermates. Among the oligodendrocyte lineage cells in the hippocampus of AD mice, fewer were mature oligodendrocytes and more were immature oligodendrocytes. Furthermore, decreased expression of SOX10, increased expression of LINGO1 and its ligands, and increased expression and activity of GSK3β might work together to induce oligodendrocyte maturation disorder in the hippocampus of AD mice. Fluoxetine treatment not only delayed the deficiencies in spatial learning and memory ability but also rescued the decrease in mature oligodendrocytes and reversed the abnormal increase in oligodendrocyte lineage cells in the hippocampus of AD mice, potentially by inhibiting the expression of LINGO1 and its ligands, inhibiting the expression and activity of GSK3β, reducing the levels of soluble Aβ40 and Aβ42, reducing β-amyloid plaques, reducing the ratio of oligodendrocytes expressing p16, promoting the expression of SOX10 in oligodendrocytes and promoting the maturation of newborn oligodendrocytes, and then increasing the number of mature oligodendrocytes in the hippocampus of AD mice.

Conclusion There is oligodendrocyte maturation disorder in the hippocampus during early AD mice. Fluoxetine exposure during early AD may delay cognitive dysfunction by affecting hippocampal oligodendrocyte generation and maturation. Early hippocampal oligodendrocyte generation and maturation in AD might be regarded as a novel therapeutic target.

1. Background

Alzheimer's disease (AD) is a devastating neurodegenerative disease predominantly associated with progressive cognitive impairment and memory impairment. More than 46 million people worldwide are affected by AD, and AD has become a serious social problem due to the associated great economic burden on society and low quality of life for families [1]. However, the pathogenesis of AD is not clearly known, and there is still no effective cure [2, 3]. Great challenges regarding AD will be faced worldwide in

the coming decades. Studies of the pathogenesis of AD and strategies to prevent AD progression in the early stage are urgently needed.

In the past two decades, the beta amyloid peptide (Aβ) toxicity hypothesis has been the most researched pathological mechanism of AD. However, the effectiveness of the treatment of AD around the Aβ toxicity hypothesis has been questioned [3, 4]. Therefore, more in-depth studies of the pathological mechanisms of AD are needed. In the early stages of AD, signaling disorders between neurons may be an important cause of memory and cognitive decline [5–7]. Signaling disorders between neurons may be due to demyelination and/or axonal degeneration and synaptic alterations [5–7]. Smith et al. found that axonal transport was decreased significantly before Tg2576 mice developed senile plaques [7]. Recent evidence and our previous study suggested that myelin breakdown and loss of myelinated fibers are associated with early-stage AD [8–10]. Demyelination disrupts brain function that is highly dependent on synchronized nerve impulses and ultimately leads to the breakdown of functional brain regions and consequent neuronal loss [11]. Therefore, demyelination may play a key role in the early alterations of AD. Oligodendrocytes, also known as myelinating glia, form the myelin of nerve fibers in the central nervous system (CNS) [12]. Compared with nerve cells, oligodendrocytes are more sensitive to ischemia and hypoxia [13]. Previous studies have indicated that β-amyloid is cytotoxic to oligodendrocytes in the AD brain [14–16] and that alterations in myelin morphology and oligodendrocyte development are present during the early stage of AD [15, 17]. As early as 2010, Desai et al. proposed that early oligodendrocyte/myelin pathology in AD mice was a novel therapeutic target [18]. Therefore, we hypothesized that oligodendrocyte changes are of great significance in the pathogenesis of AD and might be an early pathogenic factor of AD.

The hippocampus is the primary site of amyloid plaque deposition and the key structure responsible for mnemonic functions [19]. Hippocampal pathology is very relevant, especially in the early stages of AD. Our previous study reported a marked loss of myelinated fibers and myelin sheaths in the hippocampus during early AD in mice [10, 20]. In particular, Tg2576 mice showed significant decreases in myelinated fibers and myelin sheaths in the dentate gyrus before hippocampal atrophy [10]. Moreover, Desai et al. reported that myelination pattern abnormalities in the hippocampus occurred prior to the appearance of amyloid and tau pathologies in triple-transgenic AD mice, indicating that myelin abnormalities in the hippocampus might be an important factor in the etiology of AD [21]. Studies have shown that defects in the spatial learning and memory ability of AD mice are related to myelin damage in the hippocampus and that hippocampal myelin damage repair can improve their spatial learning and memory ability [22]. Oligodendrocyte changes may be a central factor related to myelin abnormalities in the hippocampus of AD. However, whether oligodendrocyte abnormalities exist in the hippocampus of those with AD is unclear. In particular, no study has quantitatively investigated oligodendrocyte changes in the hippocampus during early AD.

Studies investigating the prevention and delay of AD progression are ongoing, and treatment or intervention during early AD is considered the optimal strategy [23]. The focus of AD research has shifted from postdiagnostic treatment research to prevention and active intervention in early AD [24]. Fluoxetine,

a selective serotonin reuptake inhibitor (SSRI) antidepressant, has been shown to improve cognition and memory in AD during studies of fluoxetine for the treatment of psychiatric symptoms in AD [25–27]. Studies have shown that fluoxetine can also improve the memory and cognition of animals with AD [28, 29]. In addition, Mowla et al. reported that fluoxetine improved the cognition of patients with mild cognitive impairment (MCI) but had no effect on the cognition of AD patients [30, 31]. Animal models of AD usually simulate patients with mild to moderate AD; however, patients with AD are already in later stages of the disease upon clinical diagnosis. We hypothesized that fluoxetine might protect brain function during early AD, and the effects of fluoxetine on early pathological factors in the AD brain might be the structural basis of its brain function protection. However, the effects of fluoxetine on brain pathology (e.g., changes in myelin sheaths and oligodendrocytes) in early AD are unclear.

Whether fluoxetine affects oligodendrocytes in the hippocampus during early AD is currently unknown. The main pharmacological effects of fluoxetine are to increase the concentration of extracellular serotonin (5-HT) by inhibiting 5-HT reuptake by synapses, and the effect of 5-HT depends on its binding to its receptor [32, 33]. A previous study reported that 5-HT1A receptors are expressed in cultured oligodendrocytes at various stages [34]. There is evidence that fluoxetine activates 5-HT1A receptors (5-HT1ARs) in the brains of emotionally impaired mice and schizophrenic mice by increasing 5-HT concentrations, thereby inhibiting the expression of glycogen synthase kinase 3 (GSK3) [35, 36]. GSK3β, a subtype of GSK3, is an important negative regulator of oligodendrocyte differentiation and myelination. GSK3β inhibition not only increases the number of oligodendrocytes and oligodendrocyte precursor cells but also promotes the formation of myelin [37]. Lee et al. found that fluoxetine prevented oligodendrocyte cell death after spinal cord injury [38]. However, no study has investigated the effects of fluoxetine on oligodendrocytes in the hippocampus during early AD, and how fluoxetine affects oligodendrocytes through GSK3β in the hippocampus during early AD is unknown.

To address these questions, in the current study, we first used unbiased stereological techniques and molecular biotechnology to quantitatively investigate changes in the oligodendrocytes of the hippocampus during early AD. We then investigated whether fluoxetine improved the learning and memory abilities of AD mice by preventing the pathological changes of hippocampal oligodendrocytes during early AD. Meanwhile, we explored the possible mechanisms for the effects of fluoxetine on oligodendrocytes in the hippocampus during early AD.

2. Methods

2.1 Animals

Forty 8-month-old male amyloid precursor protein (APP)/ presenilin 1 (PS1) mice and forty 8-month-old male nontransgenic littermate mice were randomly selected. All mice were provided by the Animal Model Institute of Nanjing University and reproduced in the Experimental Animal Center at Chongqing Medical University, P. R. China. The transgenic APP/PS1 mice were randomly divided into the normal saline group (Tg+NS, n = 20) and the fluoxetine group (Tg+FLX, n = 20). The nontransgenic littermate mice were age-

matched and divided into the normal saline control group (Tg-NS, n = 20) and the fluoxetine control group (Tg-FLX, n = 20). Animal care and treatment followed the National Institute of Health Guide for the Care and Use of Laboratory Animals (NIH Publication 85-23).

2.2 Intervention programs

The two fluoxetine groups were subjected to intraperitoneal injection of fluoxetine (10 mg/kg/d) for 2 months. The two saline groups were subjected to intraperitoneal injection of the same dose of normal saline for 2 months. During the intervention, the mice were reared in a standard environment and weighed every week.

2.3 Behavioral tests

2.3.1 Open-field test

The open-field test was used to evaluate the exploratory behavior and general activity of experimental animals in the new environment [39]. After the two months of intervention, the open-field test was performed in a gray square box (36 by 36 inches). A mouse was placed in a corner of the box at the beginning of the test. The total distance traveled in the open field and the time spent in the inner squares were measured in a 300-s session. The behaviors of mice were recorded using a camera recorder placed above the box, and the data were analyzed by an observer who was blinded to the experimental design. The central area activity distance ratio (the total distance traveled in the central area divided by the total distance traveled in the open field) and the central area activity time ratio (the time spent in the central area divided by the total time spent in the open field) were used to evaluate the exploratory behavior and general activity.

2.3.2 Morris water maze test

The Morris water maze test was applied for six consecutive days to evaluate the spatial learning and memory abilities of each group [40, 41]. The hidden platform test was performed every day from the first day to the fifth day, followed by a probe trial test on the sixth day. During the hidden platform test, the mouse was placed on the platform for 10 s for adaption prior to each trial. Then, the mouse was placed in the pool at a randomly chosen starting point in one of the four quadrants. The swimming speed, escape latency, and swimming distance were recorded. If the mouse could not find the platform within 60 s, it was placed on the platform and allowed to stay there for 15 s. During the probe trial, the platform was removed. The two points that were the greatest distance from the platform were chosen as entry points. The swimming speed, the frequency of target zone crossings and the swimming time in the target zone were recorded.

2.4 Tissue processing

Ten mice from each group were chosen at random, deeply anesthetized with 1% pentobarbital sodium (0.4ml/100g) and fixed via perfusion with 4% paraformaldehyde. After perfusion, the cerebral

hemispheres were removed, and the brain masses were weighed. The right or left hemisphere was chosen at random and postfixed in 4% paraformaldehyde for more than 2 hours. Then, the tissue was embedded with optimum cutting temperature compound (OCT) medium and coronally sliced at 50-μm equidistant intervals with a cryo-ultramicrotome (Leica Microsystems, CM1950, Germany). According to the stereological sampling principle [42, 43], one of every 5 sections was systematically sampled, with the first section randomly sampled from the first 5 sections. Therefore, the section sampling fraction (ssf) was 1/5. These frozen tissue sections were used for immunohistochemical and immunofluorescence staining. The other ten mice in each group were anesthetized with 1% pentobarbital sodium (0.4 ml/100 g) and sacrificed, and fresh hippocampal brain tissue was isolated and stored at -80 °C. These tissues were used for enzyme-linked immunosorbent assay (ELISA) and Western blot analysis.

2.5 ELISA

The major protein component of AD plaques is Aβ, a 40- to 42-amino-acid peptide cleaved from APP by β-secretase and a putative γ-secretase. The levels of Aβ40 and Aβ42 in hippocampal brain tissue samples were measured with an Aβ 40 Mouse ELISA Kit (KHB3481, Invitrogen, USA) and an Aβ 42 Mouse ELISA Kit (KHB3544), respectively.

First, 50 μl of standards, controls and samples was added to 96-well plates. Second, 50 μl of Aβ40 or Aβ42 detection antibody solution was added to each well, fully mixed and incubated for 3 hours at room temperature, followed by four washes with wash buffer. Third, 100 μl anti-rabbit IgG horseradish peroxidase (HRP) was added to each well, fully mixed and incubated for 30 min at room temperature, followed by four washes with wash buffer. Fourth, 100 μl of stabilized chromogen was added to each well, fully mixed and incubated for 30 min at room temperature in the dark, and the liquid in the 96-well plates turned blue. Then, 100 μl of stop solution was added and fully mixed, and the liquid changed from blue to yellow. Finally, target protein expression in the plates was quantitatively analyzed at 450 nm.

2.6 Western blot analysis

The target proteins were measured with the following primary antibodies: anti-2‘3‘-cyclic nucleotide 3‘-phosphodiesterase (CNPase; mouse, 1:1000, ab6319, Abcam), anti-myelin basic protein (MBP; mouse, 1:1000, ab62631, Abcam), anti-NG2 (NG2; mouse, 1:1000, sc-33666, SANTA CRUZ), anti-SOX10 (SOX10; rabbit, 1:1000, ab155279, Abcam), anti-GSK3β (rabbit, 1:1000, D5C5Z, CST), anti-phosphorylated (Ser9) GSK3β (p-ser9-GSK3β; rabbit, 1:1000, D85E12, CST), anti-5-HT1AR (rabbit, 1:1000, ab85615, Abcam), anti-leucine-rich repeat and Ig domain containing 1 gene (LINGO1; rabbit, 1:1000, ab23631, Abcam), anti-myelin-associated glycoprotein (MAG; mouse, 1:1000, ab89780, Abcam), anti-myelin oligodendrocyte glycoprotein (MOG; rabbit, 1:1000, ab233549, Abcam), anti-glyceraldehyde 3-phosphate dehydrogenase (GAPDH; rabbit, 1:5000, ab8245, Abcam), anti-human gene and protein symbol ACTB/ACTB (β-actin; mouse, 1:5000, ab8226, Abcam) and anti-heat-shock protein 90 (HSP90; rabbit, 1:2000, ab203126, Abcam). The corresponding secondary antibodies for each protein were used at a dilution of 1:1000, followed by development with an ECL kit (AR1111, Boster, China).

2.7 Immunohistochemistry

Two groups of sections were randomly selected from 5 groups of sections (50 μm) per mouse; one group was used for anti-Olig2 immunohistochemistry, and another group was used for anti-CNPase immunohistochemistry. Immunohistochemistry was performed using Streptavidin/Peroxidase (SP) Link Detection Kits (sp9001 and sp9002, ZSGB-BIO, China). Briefly, the sections were rinsed for 4 ×15 min in 0.01 M phosphate-buffered solution with 0.3% Triton X-100 and 0.1% Tween 20 (PBS-T). Endogenous peroxidase activity was inhibited by incubating the sections with 3% hydrogen peroxide for 20 min. The antigen was retrieved in citrate buffer (0.01 M, pH 6.0, 99 °C) for 30 min, and nonspecific binding sites were blocked by incubating the sections with normal goat serum for 2 hours at 37 °C. Then, the primary anti-CNPase (mouse, ab6319, Abcam) and anti-Olig2 (rabbit, ab109186, Abcam) antibodies were added to the slice at a dilution of 1:500 in PBS. The tissue sections were then incubated at 4 °C for 72 hours and then rewarmed at 37 °C for 2 hours. The goat anti-mouse/rabbit immunoglobulin G secondary antibody solution was added and incubated at 37 °C for 2 hours. Then, streptavidin-HRP (S-HRP) was added and incubated for 30 min. The slices were transferred to a diaminobenzidine (DAB) solution (DAB, ZLL-9032, ZSGB) for approximately 1 min. Finally, the sections were dehydrated by sequential immersion in a gradient of ethanol solutions (70%, 80%, 90%, 100%, 100%, 100%, 10 min each) and cleared in xylene (3 × 10 min).

2.8 Immunofluorescence

A group of sections was randomly selected from three additional groups of sections per mouse. The sections were rinsed in PBS-T 4 times 15 min each as previously described and then infiltrated in 2 mol/L HCl successively for 10 min at 0 °C, 25 °C and 37 °C. After the sections were repaired in boric acid solution for 10 min, nonspecific binding sites were blocked by incubating the sections with normal goat serum for 2 hours at 37 °C. Then, the primary anti-CNPase (mouse, ab6319, Abcam), anti-Olig2 (rabbit, ab109186, Abcam), anti-SRY-related HMG-box 10 (SOX10; rabbit, ab155279, Abcam), anti-platelet-derived growth factor alpha (PDGFα; mouse, ab96569, Abcam), anti-bromodeoxyuridine (BrdU; rat, ab6326, Abcam), anti-Aβ (mouse, ab11132, Abcam) and anti-CDKN2A/p16INK4a (p16; mouse, ab201980, Abcam) antibodies were added at a dilution of 1:500 in PBS and incubated at 4 °C for 72 hours and then rewarmed at 37 °C for 2 hours. Then, secondary antibodies (1:200) were the appropriate DyLight 405, DyLight 488, and DyLight 549 (Abbkine)-conjugated antibodies. Finally, the sections were mounted on gelatin-coated slides with antifade solution to reduce fluorescence quenching.

2.9 Quantitative analyses

After immunohistochemical staining, sections were viewed using a modified Olympus BX51 microscope (Olympus, Japan). After immunofluorescence staining, sections were observed using a laser scanning confocal microscope (Nikon, Japan).

2.9.1 Estimation of the total numbers of oligodendrocyte lineage cells ($Olig2^+$ cells) in the hippocampal subregions

Using stereological analysis software (New CAST, Denmark), the numbers of Olig2$^+$ cells in the hippocampal subregions (dentate gyrus (DG), CA1, CA2-3) were counted as follows. First, at 1.25× magnification, the whole image of each section was captured using the super navigator tool of stereological analysis software (New CAST, Denmark). Second, at 4× magnification, the boundaries of the hippocampal subregions (DG, CA1 and CA2-3) were traced and drawn (Fig. 1A). Third, at 100× magnification (N.A.1.40), the counting frame was activated, and the size of the counting frame, height of the guard zone (3 μm), height of the counting zone and the area sampling fraction (asf) were set. Then, the section was automatically and randomly sampled according to the set parameters. Fourth, Olig2$^+$ oligodendrocytes in the hippocampal subregions of each section were counted at 100× magnification (N.A.1.40) [44, 45] (Fig. 1B). During counting, the average thickness of each section after staining was recorded to ensure that every section was thick enough for stereological counting. The ratio between the height of the counting zone and the average thickness of the sections represented the thickness sampling fraction (tsf). Finally, the total number of Olig2$^+$ cells in the DG, CA1 field, and CA2-3 fields of each hemisphere was estimated using an optical fractionator [42-43] as follows:

$$N = \sum Q^{-} \times \frac{1}{ssf} \times \frac{1}{asf} \times \frac{1}{tsf} \quad (1)$$

where N is the total number of Olig2$^+$ cells in the corresponding hippocampal subregions per mouse; $\sum Q^{-}$ represents the total number of Olig2$^+$ cells counted in the corresponding hippocampal subregions; *ssf* represents the slice sampling fraction (here, *ssf* is 1/5); *asf* represents the area sampling fraction (here, *asf* is 6%); and *tsf* represents the height sampling fraction calculated as the height of the counting zone/average thickness of the sections (here, the height of the counting zone is 15 μm, and the average thickness of the sections is 21.24 μm, so *tsf* is 15/21.24).

2.9.2 Estimation of the total numbers of mature oligodendrocytes (CNPase$^+$ cells) in the hippocampal subregions

Using stereological analysis software (New CAST, Denmark), the numbers of CNPase$^+$ cells in the hippocampal subregions (DG, CA1, and CA2-3) were counted as an estimation of the number of Olig2$^+$ cells in the hippocampal subregions (Fig. 1C). Here, *ssf* is 1/5; *asf* is 8%; the height of the counting zone is 15 μm, and the average thickness of sections is 22.03 μm, so *tsf* is 15/22.03.

2.9.3 Analyzing the numbers of SOX10$^+$, SOX10$^+$/PDGFα$^+$, and SOX10$^+$/CNPase$^+$ cells in the hippocampal subregions

Using confocal reconstruction technology with a laser scanning confocal microscope, we acquired images of the sections and counted the numbers of SOX10$^+$, SOX10$^+$/PDGFα$^+$, and SOX10$^+$/CNPase$^+$ cells in the hippocampal subregions.

2.9.4 Analyzing the numbers of mature or immature oligodendrocytes and newborn mature or immature oligodendrocytes in the hippocampal subregions

Using confocal reconstruction technology with a laser scanning confocal microscope, we acquired images of the sections and counted the numbers of $Olig2^+/CNPase^+$ (mature oligodendrocytes), $Olig2^+/CNPase^-$ (immature oligodendrocytes), $BrdU^+/Olig2^{+/}CNPase^+$ (newborn mature oligodendrocytes) and $BrdU^+/Olig2^+/CNPase^-$ (newborn immature oligodendrocytes) cells in the hippocampal subregions.

2.9.5 Analyzing the ratio of $p16^+/Olig2^+$ cells in the hippocampal subregions

Using confocal reconstruction technology with a laser scanning confocal microscope, we acquired images of the sections and calculated the ratio of $p16^+/Olig2^+$ cells in the hippocampal subregions.

2.10 Statistics

The results are presented as the mean (x) ± standard deviation (SD). Statistical analyses were performed using SPSS (ver. 19.0, SPSS Inc., Chicago, USA). The Shapiro-Wilk test was used to evaluate whether the group means of data were normally distributed. Repeated-measures analysis of variance (ANOVA) was used to analyze the data from the hidden platform task. One-way ANOVAs were used to compare the other data between any two groups that differed only by a single factor, such as for comparisons between the Tg-NS and Tg+NS groups, Tg-NS and Tg-FLX groups, and Tg+NS and Tg+FLX groups. A p value < 0.05 was considered an indicator of significance. The observed coefficient of variation (OCV) values and observed coefficient of error (OCE) values were calculated according to Gundersen et al. [43].

3. Results

3.1 There were no significant changes in the body weights of mice during fluoxetine intervention

No group exhibited a significant change in body weight from before to after the intervention period, and there were no significant differences in body weight between any two groups compared, such as the Tg-NS and Tg+NS groups (p = 0.866), Tg-NS and Tg-FLX groups (p = 0.649), and Tg+NS and Tg+FLX groups (p = 0.755; Fig. 2A).

3.2 There were no significant changes in the exploratory behavior or general activity of mice in the new environment during fluoxetine intervention

There were no significant differences in the central area activity time ratio or the central area distance time ratio between any two groups compared, such as the Tg-NS and Tg+NS groups (p = 0.764 & p = 0.689), Tg-NS and Tg-FLX groups (p = 0.309 & p = 0.68) , and Tg+NS and Tg+FLX groups (p = 0.808 & p = 0.448; Fig. 2B & C).

3.3 Fluoxetine delayed deficiencies in spatial learning and memory ability during early AD

Traces of the location of the mice in the hidden platform test and the probe trial test for the four groups are presented in Fig. 2D. There were no significant differences in the swimming speed between any two groups compared, such as the Tg-NS and Tg+NS groups, Tg-NS and Tg-FLX groups, and Tg+NS and Tg+FLX groups (p = 0.854, p = 0.757 & p = 0.567, respectively; Fig. 2E). The escape latency of the Tg+NS group in the hidden platform test was significantly longer than that in the Tg-NS group (p = 0.001; Fig. 2F), whereas there was no significant difference in escape latency between the Tg-NS group and Tg-FLX group (p = 0.954; Fig. 2F). The escape latency of the Tg+FLX group in the hidden platform test was significantly shorter than that of the Tg+NS group (p = 0.024; Fig. 2F). There was no significant difference in the swimming distance between the Tg-NS group and Tg+NS group in the hidden platform test (p = 0.102; Fig. 2G); however, the swimming distance of the Tg+FLX group was significantly shorter than that of the Tg+NS group in the hidden platform test (p = 0.027; Fig. 2G). The target zone frequency of the Tg+NS group was significantly lower than that of the Tg-NS group (p = 0.013; Fig. 2H), but there was no significant difference in target zone frequency between the Tg-NS group and Tg-FLX group (p = 0.266; Fig. 2H). Importantly, the target zone frequency of the Tg+NS group was significantly lower than that of the Tg+FLX group (p = 0.031; Fig. 2H). There was no significant difference in the swimming time in the target zone between any two groups, including the Tg-NS and Tg+NS groups, Tg-NS and Tg-FLX groups, and Tg+NS and Tg+FLX groups (p = 0.173, p = 0.230 & p = 0.267, respectively; Fig. 2I). There was no significant difference in the quadrant percentage time between any two groups, including the Tg-NS and Tg+NS groups, Tg-NS and Tg-FLX groups, and Tg+NS and Tg+FLX groups (p = 0.149, p = 0.095 & p = 0.596, respectively; Fig. 2J).

3.4 There were no significant changes in mouse brain mass during the fluoxetine intervention

No two groups compared showed a significant difference in brain mass, including the Tg-NS and Tg+NS groups, Tg-NS and Tg-FLX groups, and Tg+NS and Tg+FLX groups (p = 0.586, p = 0.35 & p = 0.697, respectively; Fig. 2K).

3.5 Fluoxetine rescued the decrease in mature oligodendrocytes and reversed the abnormal increase in oligodendrocyte lineage cells in the hippocampus of AD mice

3.5.1 The protein levels of CNPase and MBP in the hippocampus of AD mice

The hippocampal protein levels of CNPase and MBP (17 kDa & 21 kDa) in the Tg+NS group were significantly lower than those in the Tg-NS group (p = 0.008, p = 0.008 & p = 0.003; Fig. 3A & B). There was no significant difference in the protein levels of CNPase or MBP (17 kDa & 21 kDa) in the hippocampus between the Tg-NS group and Tg-FLX group (p = 0.839, p = 0.521 & p = 0.509; Fig. 3A & B). The hippocampal protein levels of CNPase and MBP (17 kDa & 21 kDa) in the Tg+FLX group were significantly higher than those in the Tg+NS group (p = 0.019, p = 0.015 & p = 0.002; Fig. 3A & B).

3.5.2 The total number of oligodendrocyte lineage cells ($Olig2^+$ cells) and mature oligodendrocytes ($CNPase^+$ cells) in the hippocampus

The $Olig2^+$ cells and $CNPase^+$ cells in the hippocampal subregions (CA1, CA2-3 and DG) of the four groups of mice are shown in Fig. 3C & 3D, respectively.

The total numbers of $Olig2^+$ cells and $CNPase^+$ cells in each group are presented in Table 1. In the current study, the observed variance of the individual estimate (OCE^2) was less than half of the observed interindividual variance (OCV^2), indicating that the sampling was considered optimal.

The total numbers of $Olig2^+$ cells in the CA1 field, CA2-3 fields and DG of the Tg+NS mice were significantly greater than those in the respective areas of the Tg-NS mice ($p = 0.037$, $p = 0.002$ & $p < 0.001$; Fig. 3E). There were no significant differences in the total numbers of $Olig2^+$ cells in the CA1 field, CA2-3 fields or DG between the Tg-NS mice and Tg-FLX mice ($p = 0.123$, $p = 0.844$ & $p = 0.320$; Fig. 3E). There were no significant differences in the total numbers of $Olig2^+$ cells in the CA1 field between the Tg+NS mice and Tg+FLX mice; however, the total numbers of $Olig2^+$ cells in the CA2-3 fields and DG of the Tg+FLX mice were significantly lower than those in the same areas of the Tg+NS mice ($p = 0.201$, $p = 0.021$ & $p = 0.003$; Fig. 3E).

The total numbers of $CNPase^+$ cells in the CA1 field, CA2-3 fields and DG of the Tg+NS mice were significantly lower than those in the respective areas of the Tg-NS mice ($p = 0.003$, $p = 0.012$ & $p < 0.001$; Fig. 3F). There were no significant differences in the total numbers of $CNPase^+$ cells in the CA1 field, CA2-3 fields or DG between the Tg-NS mice and Tg-FLX mice ($p = 0.374$, $p = 0.386$ & $p = 0.800$; Fig. 3F). The total numbers of $CNPase^+$ cells in the CA1 field, CA2-3 fields and DG of the Tg+FLX mice were significantly greater than those in the respective areas of the Tg+NS mice ($p = 0.001$, $p = 0.005$ & $p < 0.001$; Fig. 3F).

3.5.3 The densities of mature $Olig2^+$ and immature $Olig2^+$ cells in the hippocampus

The $Olig2^+/CNPase^+$ (mature $Olig2^+$) and $Olig2^+/CNPase^-$ (immature $Olig2^+$) cells in the hippocampus (CA1, CA2-3 and DG) of the four groups are shown in Fig. 3G.

The densities of $Olig2^+/CNPase^+$ cells in the CA1 field, CA2-3 fields and DG of the Tg+NS mice were significantly lower than those in the same areas of the Tg-NS mice ($p < 0.001$, $p = 0.001$ & $p = 0.012$; Fig. 3H). The density of $Olig2^{+/}CNPase^+$ cells in the CA1 field of the Tg-FLX mice was significantly lower than that in the CA1 field of the Tg-NS mice; however, there were no significant differences in the densities of $Olig2^{+/}CNPase^+$ cells in the CA2-3 fields or DG between the Tg-NS mice and Tg-FLX mice ($p = 0.015$, $p = 0.229$ & $p = 0.869$; Fig. 3H). The densities of $Olig2^+/CNPase^+$ cells respectively in the CA1 field, CA2-3 fields and DG of the Tg+FLX mice were significantly great than those in the same regions of the Tg+NS mice ($p = 0.007$, $p = 0.011$ & $p = 0.014$; Fig. 3H).

The densities of $Olig2^+/CNPase^-$ cells in the CA1 field, CA2-3 fields and DG of the Tg+NS mice were significantly greater than those in the same regions of the Tg-NS mice ($p = 0.001$, $p < 0.001$ & $p < 0.001$; Fig. 3I). There were no significant differences in the densities of $Olig2^+/CNPase^-$ cells in the CA1 field,

CA2-3 fields or DG between the Tg-NS mice and Tg-FLX mice ($p = 0.147$, $p = 0.594$ & $p = 0.863$; Fig. 3I). The densities of $Olig2^+/CNPase^-$ cells in the CA1 field, CA2-3 fields and DG of the Tg+FLX mice were significantly lower than those of the Tg+NS mice ($p = 0.009$, $p < 0.001$ & $p = 0.001$; Fig. 3I).

The ratios of $CNPase^+$ cells to $Olig2^+$ cells in the CA1 field, CA2-3 fields and DG of the Tg+NS mice were significantly lower than those of the Tg-NS mice ($p < 0.001$, $p < 0.001$ & $p < 0.001$; Fig. 3J). The ratio of $CNPase^+$ cells to $Olig2^+$ cells in the CA2-3 fields of the Tg-FLX mice was significantly lower than that in the same region of the Tg-NS mice; however, there were no significant differences in the ratios of $CNPase^+$ cells to $Olig2^+$ cells in the CA1 field or DG between the Tg-NS mice and Tg-FLX mice ($p = 0.01$, $p = 0.362$ & $p = 0.066$; Fig. 3J). The ratios of $CNPase^+$ cells to $Olig2^+$ cells in the CA1 field, CA2-3 fields and DG of the Tg+FLX mice were significantly greater than those of the Tg+NS mice ($p < 0.001$, $p = 0.002$ & $p < 0.001$; Fig. 3J).

3.6 Fluoxetine not only increased SOX10 protein expression in mature oligodendrocytes but also promoted the maturation of newborn oligodendrocytes in the hippocampus of AD mice

3.6.1 The protein levels of NG2 and SOX10 in the hippocampus

There were no significant differences in the hippocampal protein levels of NG2 or SOX10 between any two groups compared, including between the Tg-NS and Tg+NS groups, Tg-NS and Tg-FLX groups, and Tg+NS and Tg+FLX groups ($p = 0.975$, $p = 0.447$, $p = 0.706$, $p = 0.679$, $p = 0.431$ & $p = 0.839$, respectively; Fig. 4A & B).

3.6.2 The protein level of SOX10 in hippocampal oligodendrocytes

$SOX10^+$ cells in the hippocampus (CA1, CA2-3 and DG) of the four groups are shown in Fig. 4C. There were no significant differences in the density of $SOX10^+$ cells in the CA1 field between any two groups compared, including between the Tg-NS and Tg+NS groups, Tg-NS and Tg-FLX groups, and Tg+NS and Tg+FLX groups ($p = 0.24$, $p = 0.764$ & $p = 0.550$; Fig. 4D), and there were no significant differences in the density of $SOX10^+$ cells in the CA2-3 fields or DG between the Tg-NS group and Tg-FLX group ($p = 0.861$ & $p = 0.888$; Fig. 4D). However, the densities of $SOX10^+$ cells in the CA2-3 fields and DG of the Tg+NS mice were significantly lower than those of the Tg-NS mice ($p = 0.012$ & $p = 0.016$; Fig. 4D), and the densities of $SOX10^+$ cells in the CA2-3 fields and DG of the Tg+FLX mice were significantly higher than those of the Tg+NS mice ($p = 0.004$ & $p = 0.009$; Fig. 4D).

The $SOX10^+/PDGF\alpha^+$ cells in the hippocampus (CA1, CA2-3 and DG) of the four groups are shown in Fig. 4E. There were no significant differences in the density of $SOX10^+/PDGF\alpha^+$ cells in the CA1 field or CA2-3 fields between any two groups compared, including between the Tg-NS and Tg+NS groups, Tg-NS and Tg-FLX groups, and Tg+NS and Tg+FLX groups ($p = 0.791$, $p = 0.43$, $p = 0.43$, $p = 0.217$, $p = 0.53$ & $p = 0.277$; Fig. 4F). The $SOX10^+/PDGF\alpha^+$ cell density in the DG of the Tg+NS mice was significantly lower than that in the DG of the Tg-NS mice; however, there were no significant differences in $SOX10^+$ cell density in the

CA2-3 fields or DG between the Tg-NS and Tg-FLX groups or between the Tg+NS and Tg+FLX groups (p = 0.028, p = 0.865 & p = 0.055; Fig. 4F).

The $SOX10^+/CNPase^+$ cells in the hippocampus (CA1, CA2-3 and DG) of the four groups are shown in Fig. 4G. There were no significant differences in $SOX10^+/CNPase^+$ cell density in the CA1 field or DG between any two groups compared, including between the Tg-NS and Tg+NS groups, Tg-NS and Tg-FLX groups, and Tg+NS and Tg+FLX groups (p = 0.756, p = 0.357, p = 0.756, p = 0.194, p = 0.882 & p = 0.245; Fig. 4H). There were no significant differences in $SOX10^+/CNPase^+$ cell density in the CA2-3 fields between the Tg-NS mice and Tg-FLX mice (p = 0.400; Fig. 4H). However, the density of $SOX10^{+/}CNPase^+$ cells in the CA2-3 fields of the Tg+NS mice was significantly lower than that in the CA2-3 fields of the Tg-NS mice, and the density of $SOX10^+/CNPase^+$ cells in the CA2-3 fields of the Tg+FLX mice was significantly greater than that in the CA2-3 fields of the Tg+NS mice (p = 0.028 & p = 0.039; Fig. 4H).

3.6.3 Newborn oligodendrocytes in the hippocampus

The $BrdU^+/Olig2^+/CNPase^+$ (newborn mature $Olig2^+$) cells and $BrdU^+/Olig2^+/CNPase^-$ (newborn immature $Olig2^+$) cells in the hippocampus (CA1, CA2-3 and DG) of the four groups of mice are shown in Fig. 4I.

There were no significant differences in $BrdU^+/Olig2^+/CNPase^+$ cell density in the CA1 field between any two groups compared, including between the Tg-NS and Tg+NS groups, Tg-NS and Tg-FLX groups, and Tg+NS and Tg+FLX groups (p = 0.751, p = 0.307 & p = 0.165; Fig. 4J). The density of $BrdU^+/Olig2^+/CNPase^+$ cells in the CA2-3 fields of the Tg-FLX mice was significantly greater than that in the Tg-NS mice; however, there were no significant differences in $BrdU^+/Olig2^+/CNPase^+$ cell density in the CA2-3 fields between the Tg-NS and Tg+NS groups or between the Tg+NS and Tg+FLX groups (p = 0.04, p = 0.086 & p = 0.111; Fig. 4J). Furthermore, there were no significant differences in $BrdU^+/Olig2^+/CNPase^+$ cell density in the DG between the Tg-NS mice and Tg-FLX mice (p = 0.132; Fig. 4J). However, the density of $BrdU^+/Olig2^+/CNPase^+$ cells in the DG of the Tg+NS mice was significantly lower than that in the DG of the Tg-NS mice, and the density of $BrdU^+/Olig2^+/CNPase^+$ cells in the DG of the Tg+FLX mice was significantly higher than that in the DG of Tg+NS mice (p < 0.001 & p = 0.015; Fig. 4J).

There were no significant differences in $BrdU^+/Olig2^+/CNPase^-$ cell density in the CA1 field between any two groups compared, including between the Tg-NS and Tg+NS groups, Tg-NS and Tg-FLX groups, and Tg+NS and Tg+FLX groups (p = 0.553, p = 0.473 & p = 0.732; Fig. 4K). There were no significant differences in $BrdU^+/Olig2^+/CNPase^+$ cell density in the CA2-3 fields or DG between the Tg-NS and Tg-FLX groups or between the Tg-NS and Tg+NS groups (p = 0.081, p = 0.383, p = 0.055 & p = 0.579; Fig. 4K). However, the densities of $BrdU^+/Olig2^+/CNPase^+$ cells in the CA2-3 fields and DG of the Tg+FLX mice were significantly lower than those in the same regions of the Tg+NS mice (p = 0.021 & p = 0.008; Fig. 4K).

3.7 Fluoxetine reduced the levels of soluble Aβ40 and Aβ42, the expression of β-amyloid plaques and the ratio of oligodendrocytes expressing p16 in the hippocampus of AD mice

3.7.1 Aβ40, Aβ42 and amyloid plaques in the hippocampus

The levels of Aβ40 and Aβ42 in the hippocampus of the Tg+NS mice were significantly higher than those in the hippocampus of the Tg-NS mice ($p < 0.001$ & $p < 0.001$; Fig. 5A). However, there were no significant differences in Aβ40 or Aβ42 levels in the hippocampus between the Tg-NS mice and Tg-FLX mice ($p = 0.991$ & $p = 0.387$; Fig. 5A). The levels of Aβ40 and Aβ42 in the hippocampus of the Tg+NS mice were significantly lower than those in the hippocampus of the Tg+FLX mice ($p = 0.006$ & $p = 0.018$; Fig. 5A).

As shown in Fig. 5B, no amyloid plaques were found in the hippocampus of the Tg-NS and Tg-FLX mice. In contrast, many large amyloid plaques were observed in the hippocampus of the Tg+NS and Tg+FLX mice, and there were fewer amyloid plaques in the hippocampus of the Tg+FLX mice than in those of the Tg+NS mice (Fig. 5B). In addition, larger amyloid plaques were found in the hippocampus of the Tg+NS mice than in those of the Tg+FLX mice (Fig. 5B).

3.7.2 The protein level of p16 in hippocampal oligodendrocytes

The $p16^+/Olig2^+$ cells in the hippocampus (CA1, CA2-3 and DG) of the four groups are shown in Fig. 5C. The $p16^+/Olig2^+$ cell ratios in the CA1 field, CA2-3 fields and DG of the Tg+NS mice were significantly greater than those in the same hippocampal regions of the Tg-NS mice ($p = 0.004$, $p = 0.003$ & $p = 0.01$; Fig. 5D). There were no significant differences in $p16^+/Olig2^+$ cell ratios in the CA1 field, CA2-3 fields or DG between the Tg-NS and Tg-FLX groups ($p = 0.655$, $p = 0.058$ & $p = 0.43$; Fig. 5D). Furthermore, there was no significant difference in $p16^+/Olig2^+$ cell ratio in the CA1 field between the Tg+NS mice and Tg+FLX mice; however, the $p16^{+/}Olig2^+$ cell ratios in the CA2-3 fields and DG of the Tg+FLX mice were significantly lower than those in the same regions of the Tg+NS mice ($p = 0.152$, $p = 0.018$ & $p = 0.024$; Fig. 5D).

3.8 Fluoxetine inhibited the protein expression and activity of GSK3β and the protein expression of LINGO1 and its ligands MAG and MOG in the hippocampus of AD mice but did not affect 5-HT1AR protein expression

3.8.1 The protein levels of GSK3β in the hippocampus

The expression of hippocampal GSK3β protein in the Tg+NS group was significantly greater than that in the Tg-NS group ($p < 0.001$; Fig. 5E & F). However, there was no significant difference in hippocampal GSK3β protein expression between the Tg-NS group and Tg-FLX group ($p = 0.591$; Fig. 5E & F). Finally, hippocampal GSK3β protein expression in the Tg+FLX group was significantly lower than that in the Tg+NS group ($p < 0.001$; Fig. 5E & F).

3.8.2 The protein levels of p-S9-GSK3β in the hippocampus

The expression of hippocampal p-S9-GSK3β protein in the Tg+NS group was significantly lower than that in the Tg-NS group ($p = 0.004$; Fig. 5E & F), but there was no significant difference in hippocampal p-S9-

GSK3β protein expression between the Tg-NS group and Tg-FLX group (p = 0.641; Fig. 5E & F). Importantly, the Tg+FLX group had significantly higher hippocampal p-S9-GSK3β protein expression than the Tg+NS group mice (p = 0.037; Fig. 5E & F).

3.8.3 The protein levels of 5-HT1AR in the hippocampus

There was no significant difference in 5-HT1AR protein expression in the hippocampus between any two groups compared, including between the Tg-NS and Tg+NS groups, Tg-NS and Tg-FLX groups, and Tg+NS and Tg+FLX groups (p = 0.595, p = 0.489 & p = 0.31; Fig. 5E & F).

3.8.4 The protein levels of LINGO1, MAG and MOG in the hippocampus

LINGO1, MAG and MOG protein levels in the hippocampus of the Tg+NS mice were significantly greater than those in the hippocampus of the Tg-NS mice (p = 0.008, p = 0.035 & p = 0.042; Fig. 5E & F). There were no significant differences in hippocampal LINGO1, MAG or MOG protein expression between the Tg-NS group and Tg-FLX group (p = 0.34, p = 0.463 & p = 0.457; Fig. 5E & F). Finally, hippocampal protein expression of LINGO1, MAG and MOG in the Tg+FLX group was significantly lower than that in the Tg+NS group (p = 0.018, p = 0.003 & p = 0.016; Fig. 5E & F).

4. Discussion

Alzheimer's disease (AD) is a central nervous system (CNS) degenerative disease predominantly associated with progressive cognitive impairment and memory impairment. Globally, an increasing number of people suffer from serious intellectual disability; however, there is still no effective treatment method [2, 3].

Fluoxetine, a selective serotonin reuptake inhibitor (SSRI) antidepressant, has been shown to improve cognition and memory in AD during studies of fluoxetine for the treatment of psychiatric symptoms of AD [25–27]. Marcussen et al. reported that low-dose and long-term intraperitoneal injections of fluoxetine in Wistar rats increased neurogenesis and improved cognitive behavior [46]. In recent years, an increasing number of studies have expressed that moving the treatment time window to an early stage is an effective way to prevent AD [23, 24]. A new clinical study reported that long-term SSRI treatment delayed the progression from mild cognitive impairment (MCI) to AD [47]. Therefore, in our present study, we used a low-dose (10 mg/kg/d) and long-term (2 months) intraperitoneal injection of fluoxetine in young amyloid precursor protein (APP)/ presenilin 1 (PS1) transgenic AD mice without cognitive impairment and investigated the effects of fluoxetine in the early stages of AD. We found that there was no significant difference in open-field test performance between the transgenic AD mice and nontransgenic littermates or between the groups treated with normal saline and those treated with fluoxetine. The open-field test was used to evaluate the exploratory behavior and general activity of experimental animals in a new environment [39]. Our results indicated that there was no decline in exploratory behavior or general activity of AD mice in a new environment and that fluoxetine had no adverse effects on activity. However, in the Morris water maze, the escape latency of the transgenic AD mice was significantly longer than that

of the nontransgenic littermates, and the platform-crossing frequency of the transgenic AD mice was significantly lower than that of the nontransgenic littermates. Moreover, among the nontransgenic littermates, there were no significant differences in escape latency or platform-crossing frequency in the Morris water maze test between those treated with normal saline and those treated with fluoxetine; however, among the transgenic AD mice, the escape latency of fluoxetine-treated mice was significantly shorter than that of normal saline-treated mice. The Morris water maze test was used to evaluate spatial learning and memory abilities [40, 41], and our results indicated that fluoxetine treatment partly delayed the deficiencies in spatial learning and memory ability in mice in the early stages of AD.

We then sought to examine the mechanism by which fluoxetine prevents the progression of AD. Oligodendrocyte injury and demyelination disrupt brain function [11] Behrendt et al. reported dynamic changes in myelin aberrations in the white matter in AD mice and patients [48]. By measuring the relationship between the attenuation of myelin density and AD damage, Sjöbeck et al. confirmed that myelin sheath changes were some of the most obvious histopathological changes in AD [49]. Using unbiased stereology methods, our previous studies observed damage to myelinated fibers in the white matter and hippocampus during early AD in mice [9, 10]. In particular, a significant decrease in the total length of myelinated fibers in the dentate gyrus (DG) was detected before hippocampal atrophy in Tg2576 mice [10]. This evidence indicates that demyelination plays a key role in the early alterations of AD. Studies have shown that defects in the spatial learning and memory ability of AD mice are related to myelin damage in the hippocampus and that repair of myelin damage in the hippocampus can improve spatial learning and memory [22]. Oligodendrocytes are myelinating cells in the CNS that are diffusely distributed within the hippocampus. In this study, we first investigated changes in oligodendrocytes in the hippocampus of mice in the early stages of AD. A variety of marker proteins, such as Olig2, anti-2‘3‘-cyclic nucleotide 3‘-phosphodiesterase (CNPase) and myelin basic protein (MBP), are expressed in oligodendrocyte development and myelination. Olig2 is the key to fate determination and the early differentiation of the oligodendrocyte lineage. Previous studies have shown that Olig2 knockout mice cannot produce oligodendrocyte lines in the CNS and that Olig2 expression gradually decreases during the period of maturity until it is no longer expressed [50, 51]. CNPase is the earliest known myelin-specific protein to be synthesized by developing oligodendrocytes, and CNPase expression gradually increases during maturation [52, 53]. MBP is an important component of the myelin sheath and plays an important role in maintaining its structural integrity [12]. In this study, we semiquantitatively analyzed the protein levels of CNPase and MBP in the hippocampus of AD mice. We observed that the levels of CNPase and MBP in the hippocampus of the transgenic AD mice were significantly lower than those in the hippocampus of the nontransgenic littermates. In addition, we used an anti-Olig2 antibody to label the oligodendrocyte lineage cells and an anti-CNPase antibody to label the mature oligodendrocytes and counted the total numbers of these cells using unbiased three-dimensional quantitative stereology methods. Here, the total numbers of $Olig2^+$ cells in the CA1 field, CA2-3 fields and DG were significantly higher in the transgenic AD mice than in the nontransgenic littermates; meanwhile, the total numbers of $CNPase^+$ cells in the CA1 field, CA2-3 fields and DG were significantly lower in the transgenic AD mice than in the nontransgenic littermate mice. The results indicated that AD mice with cognitive impairment

exhibited an abnormal increase in the number of oligodendrocyte lineage cells ($Olig2^+$ cells) in the hippocampus but a decrease in the levels of oligodendrocyte maturation markers (CNPase and MBP) and the number of mature oligodendrocytes ($CNPase^+$ cells) in the hippocampus. Then, using double-labeling immunofluorescence, we observed that the densities of $Olig2^+/CNPase^+$ cells in the CA1 field, CA2-3 fields and DG were significantly lower in the transgenic AD mice than in the nontransgenic littermates; meanwhile, the densities of $Olig2^+/CNPase^-$ cells in the CA1 field, CA2-3 fields and DG were significantly higher. The results further indicated that AD mice with cognitive impairment had significantly more immature oligodendrocytes ($Olig2^+/CNPase^-$ cells) but fewer mature oligodendrocytes ($Olig2^+/CNPase^+$ cells) in the hippocampus than nontransgenic littermates. Moreover, the ratios of mature oligodendrocytes to oligodendrocyte lineage cells in the CA1 field, CA2-3 fields and DG were significantly lower in the transgenic AD mice than in the nontransgenic littermate mice. Thus, AD mice with cognitive impairment had more hippocampal oligodendrocyte lineage cells than nontransgenic littermates, and among the oligodendrocyte lineage cells in the AD mouse hippocampus, fewer were mature oligodendrocytes and more were immature oligodendrocytes. Since there were oligodendrocyte abnormalities and demyelination in the hippocampus of AD mice, we sought to determine whether fluoxetine treatment could improve these oligodendrocyte abnormalities and demyelination in the hippocampus of AD mice. Previous studies have shown that fluoxetine might be able to prevent oligodendrocyte cell death after spinal cord injury [38] and ameliorate myelination deficits in mice with multiple system atrophy [54]. In this study, we observed that the levels of CNPase and MBP in the hippocampus were significantly higher in the fluoxetine-treated transgenic AD mice than in the normal saline-treated transgenic AD mice, indicating that fluoxetine treatment induced the expression of oligodendrocyte-related proteins, such as MBP and CNPase, and myelination in the hippocampus of AD mice. In addition, after fluoxetine exposure, there were no significant differences in the total numbers of $Olig2^+$ cells, total numbers of $CNPase^+$ cells, densities of $Olig2^+/CNPase^+$ cells or densities of $Olig2^+/CNPase^-$ cells in the CA1 field, CA2-3 fields or DG between the fluoxetine-treated nontransgenic littermate mice and the normal saline-treated nontransgenic littermate mice, but the ratio of mature oligodendrocytes to oligodendrocyte lineage cells in the CA2-3 fields was significantly lower in the fluoxetine-treated nontransgenic littermate mice than in the normal saline-treated nontransgenic littermate mice. However, the total numbers of $CNPase^+$ cells and densities of $Olig2^+/CNPase^+$ cells in the CA1 field, CA2-3 fields and DG were significantly greater in the fluoxetine-treated transgenic AD mice than in those given normal saline; in contrast, the total numbers of $Olig2^+$ cells and densities of $Olig2^+/CNPase^-$ cells in the hippocampus were significantly lower in the fluoxetine-treated transgenic AD mice than in those given normal saline. These results indicated that, in normal mice, fluoxetine mildly decreased the ratio of mature oligodendrocytes to oligodendrocyte lineage cells in the hippocampus; however, in AD mice, fluoxetine not only rescued the decrease in mature oligodendrocytes but also reversed the generation of abnormal oligodendrocytes in the hippocampus of AD mice.

We then sought to determine the reason for the changes in oligodendrocytes in the hippocampus of AD mice and how fluoxetine affects these changes. Regarding the loss of mature oligodendrocytes in the

hippocampus of AD mice, we speculated two possible reasons for the changes in oligodendrocytes: 1. dysfunction in oligodendrocyte development and 2. death of mature oligodendrocytes. The development of oligodendrocytes involves several processes: proliferation, differentiation and maturation. NG2 is a marker that reflects the proliferation of oligodendrocytes [55], and SOX10 plays a key role in the maturation of oligodendrocytes and myelination [56]. In this study, NG2 protein expression in the hippocampus did not differ between AD transgenic mice and littermate controls, and fluoxetine treatment had no effect on NG2 protein expression in the hippocampus of AD mice. However, AD mice had significantly lower densities of $SOX10^+$ cells in the CA2-3 fields and DG than nontransgenic littermate mice; meanwhile, the density of $SOX10^+$/platelet-derived growth factor alpha $(PDGF\alpha)^+$ cells in the DG and the density of $SOX10^+/CNPase^+$ cells in the CA2-3 fields were significantly lower in the transgenic AD mice than in the nontransgenic littermate mice. Fluoxetine treatment significantly increased the densities of $SOX10^+$ cells in the CA2-3 fields and DG of AD mice, as well as the density of $SOX10^+/CNPase^+$ cells in the CA2-3 fields. Thus, AD mice with cognitive impairment exhibited varying degrees of reductions in $SOX10^+$ cell density and SOX10 protein expression in mature and immature oligodendrocytes in the hippocampus, and fluoxetine treatment increased SOX10 protein expression in mature oligodendrocytes. Taken together, these data indicate that that maturation of oligodendrocytes in the hippocampus of AD mice might be impaired. Behrendt et al. reported increased expression of $BrdU^+/Olig2^+$ cells and $BrdU^+/NG2^+$ cells in the white matter of APP/PS1 transgenic AD mice and hypothesized that amyloidosis could induce excessive proliferation of oligodendrocytes [48]. However, Kamphuis et al. reported that none of the newborn cells in the cortex of APP/PS1 transgenic AD mice had differentiated into oligodendrocytes and suggested that amyloid plaque deposition did not affect oligodendrocyte proliferation [57]. In this study, we used anti-Olig2, anti-CNPase and anti-BrdU antibodies to label newborn oligodendrocyte lineage cells, including newborn immature oligodendrocytes and newborn mature oligodendrocytes, in the hippocampus of APP/PS1 transgenic AD mice. We found that the densities of $BrdU^+/Olig2^+/CNPase^+$ cells in the CA2-3 fields and DG were lower in the AD mice than in the littermates, further indicating that oligodendrocytes failed to mature in the hippocampus of AD mice. Combined with previous studies, our observations led us to speculate that impaired oligodendrocyte maturation in the hippocampus might be a key reason for the loss of mature oligodendrocytes in the hippocampus of AD mice. Fluoxetine treatment significantly increased the densities of $BrdU^+/Olig2^+/CNPase^+$ cells in the DG of AD mice; in contrast, fluoxetine treatment significantly decreased the densities of $BrdU^+/Olig2^+/CNPase^-$ cells in the DG and CA2-3 of AD mice. These results further indicated that fluoxetine rescued failed oligodendrocyte maturation in the hippocampus of AD mice. Our results showed that oligodendrocyte abnormalities and demyelination in the hippocampus of AD could be improved, potentially representing an important structural basis for the protective effects of fluoxetine on AD progression. Oligodendrocytes in the hippocampus could be an important target in the prevention of AD progression from the early stages.

Next, we examined the cause of the oligodendrocyte maturation impairment in the hippocampus of AD mice and the mechanism by which fluoxetine rescued it. Previous studies have reported that β-amyloid is

cytotoxic to oligodendrocytes and induces oligodendrocyte death [14, 16]. In this study, we analyzed β-amyloid in the hippocampus. We observed that the levels of beta amyloid peptide 40 (Aβ40) and Aβ42 in the hippocampus of the transgenic AD mice were significantly higher than those in the hippocampus of the nontransgenic littermate mice. No amyloid plaques were found in the hippocampus of the nontransgenic littermate mice, whereas many large amyloid plaques were observed in the hippocampus of the transgenic AD mice. After fluoxetine exposure, there was less Aβ40, Aβ42 and amyloid plaque formation in the hippocampus of the fluoxetine-treated transgenic AD mice than in the hippocampus of transgenic AD mice given normal saline. The results indicated that fluoxetine reduced β-amyloid in the hippocampus of early AD mice, which is consistent with previous studies [58–59]. The decrease in β-amyloid might reduce the cytotoxicity to oligodendrocytes and prevent oligodendrocyte death in the hippocampus of AD mice. A previous study reported that β-amyloid induced p16 and p21 protein expression in oligodendrocyte progenitor cells and then induced oligodendrocyte progenitor cell senescence [60]. In this study, the ratio of oligodendrocytes expressing p16 in the hippocampus was higher in AD mice with cognitive impairment than in nontransgenic littermate controls. However, fluoxetine exposure decreased the ratio of oligodendrocytes expressing p16 in the hippocampus of AD mice. We speculated that oligodendrocyte senescence might result in the loss of the ability of these cells to mature and that fluoxetine could inhibit the expression of p16 in oligodendrocytes, thereby promoting the maturation of oligodendrocytes in the hippocampus of AD mice. In addition, glycogen synthase kinase 3β (GSK3β) is an important negative regulator of oligodendrocyte differentiation and myelination [37]. In this study, the protein level of GSK3β in the hippocampus of transgenic AD mice was significantly higher than that in the hippocampus of nontransgenic littermate mice; however, the protein level of GSK3β phosphorylated at Ser9 in the hippocampus of transgenic AD mice was significantly lower than that of nontransgenic littermate mice. Compared to normal saline treatment, fluoxetine treatment decreased the protein level of GSK3β and increased the protein level of GSK3β phosphorylated at Ser9 in the hippocampus of the AD mice. Thus, increased GSK3β expression and activity might be another reason for the maturation disorder of oligodendrocytes in the hippocampus of AD mice, and fluoxetine might promote oligodendrocyte maturation by inhibiting the expression and activity of GSK3β in the hippocampus of AD mice. How does fluoxetine inhibit the expression and activity of GSK3β in the hippocampus of AD mice? The main pharmacological effects of fluoxetine are to increase the concentration of extracellular serotonin (5-HT) by inhibiting the reuptake of 5-HT by synapses, and the effect of 5-HT depends on its binding to its receptor [32, 33]. There is evidence that fluoxetine activates 5-HT1A receptors (5-HT1ARs) in the brains of emotionally impaired mice and schizophrenic mice by increasing 5-HT concentrations, thereby inhibiting the expression of GSK3 [35, 36]. In this study, there were no significant differences in hippocampal 5-HT1AR protein expression between the transgenic AD mice and nontransgenic littermate mice or between the normal saline groups and fluoxetine groups. Our results indicated that there was no decrease in the expression of the 5-HT1AR in the hippocampus of AD mice, and fluoxetine had no effect on the expression of the 5-HT1AR in the hippocampus of AD mice. In other words, fluoxetine inhibited the protein expression and activity of GSK3β but not by increasing the levels of 5-HT1AR. Therefore, we explored another target. Leucine-rich repeat and Ig domain containing 1 gene (LINGO1) is a component of the Nogo-66 receptor/p75 signaling complex, which is an anther

negative regulator of oligodendrocyte differentiation and myelination [61, 62]. A previous study reported that antagonized LINGO1 ameliorated myelin impairment and spatial memory deficits in the early stage of the disease in 5XFAD transgenic mice [22]. In our study, hippocampal LINGO1 protein expression was significantly higher in the transgenic AD mice than in the nontransgenic littermate mice. However, fluoxetine-treated AD mice expressed lower levels of hippocampal LINGO1 protein than those treated with normal saline. Myelin-associated glycoprotein (MAG) and myelin oligodendrocyte glycoprotein (MOG) are the ligands of LINGO1 [61]. In this study, the protein levels of MAG and MOG in the hippocampus of the transgenic AD mice were significantly higher than those in the hippocampus of the nontransgenic littermate mice, but fluoxetine decreased the protein levels of MAG and MOG in the hippocampus of AD mice. A previous study reported that antagonizing LINGO1 inhibited the activity of GSK3 [63]. We speculated that the high expression of LINGO1 and its ligands MAG and MOG might be an important reason for the high expression and activity of GSK3β in the hippocampus of AD mice and may affect the maturation of oligodendrocytes. Fluoxetine might inhibit the expression and activity of GSK3β in the hippocampus of AD mice by inhibiting the expression of LINGO1 and its ligands, thereby promoting oligodendrocyte maturation in the hippocampus of AD mice.

5. Conclusion

In addition to hippocampal demyelination, hippocampal oligodendrocyte abnormalities (such as the abnormal proliferation of immature oligodendrocytes and decrease in mature oligodendrocytes) were shown to play key roles in the early alterations of AD. Fluoxetine exposure during early AD not only rescued the decrease in mature oligodendrocytes but also reversed the abnormal oligodendrocyte generation in the hippocampus of AD mice by inhibiting the expression of LINGO1 and its ligands, inhibiting the expression and activity of GSK3β, reducing Aβ, inhibiting oligodendrocyte senescence, promoting the expression of SOX10 and then increasing mature oligodendrocytes in the hippocampus of AD model mice. Fluoxetine might be a safe and effective medication for preventing or delaying the progression of AD, and early oligodendrocyte pathology in AD might be regarded as a novel therapeutic target.

Abbreviations

5HT1AR	hydroxyptamine 1A receptor
Aβ	Beta amyloid peptide
AD	Alzheimer's disease
ANOVA	Analysis of variance
APP	Amyloid precursor protein
BrdU	bromo-2'-deoxyuridine
CNPase	2’ 3’-cyclic nucleotide 3’-phosphodiesterase
DAB	Diaminobenzidine
DG	Dentate gyrus
ELISA	Enzyme linked immunosorbent assay
FLX	Fluoxetine hydrochloride
GAPDH	Glyceraldehyde 3-phosphate dehydrogenase
GSK-3β	Glycogen synthase kinase-3β
HSP90	Heat-shock protein 90
LINGO1	Leucine-rich repeat and Ig domain containing 1 gene
LSD	Least significant difference
MAG	Myelin-associated glycoprotein
MBP	Myelin basic protein
MCI	Mild cognitive impairment
MOG	Myelin oligodendrocyte glycoprotein
NS	Normal saline
OCE	Observed coefficient of error
OCT	Optimal cutting temperature
OCV	Observed coefficient of variation
Olig2	Oligodendrocyte transcription factor 2
PBS	Phosphate buffered solution
PDGFα	Platelet-derived growth factor alpha
p-S9-GSK3β	Phosphorylated (Ser9) glycogen synthase kinase-3β
PS	Presenilin

SOX10	SRY-related HMG-box 10
SSRI	Selective serotonin reuptake inhibitor

Declarations

Ethics approval and consent to participate: This study was approved by the Animal Care and Research Committee of Chongqing Medical University, China.

Consent for publication: Not applicable.

Competing interests: The authors declare that they have no competing interests.

Availability of data and materials: The datasets generated during and/or analyzed during the present study are available from the corresponding author on reasonable request.

Authors' contributions: Conception and design of the study: Yi Zhang, Feng-lei Chao, and Yong Tang; Acquisition and analysis of data: Yi Zhang, Chun-ni Zhou, Lin Jiang, and Feng-lei Chao; Drafting of a significant portion of the manuscript or figures: Yi Zhang, Feng-lei Chao; Lei Zhang, Chun-ni Zhou, Lin Jiang, Jing Tang, Jin-hua Fan, Xiao-yun Dou, and Yong Tang.

Funding: This work was supported by the National Natural Science Foundation of China (NSFC, 81671259; NSFC, 81801269).

Acknowledgements: Not applicable.

References

1. Alzheimer's Association. 2016 Alzheimer's disease facts and figures. Alzheimers Dement. 2016; 12(4): 459-509.
2. Goedert M, Spillantini MG. A century of Alzheimer's disease. Science. 2006; 314: 777-781.
3. Querfurth HW, LaFerla FM. Alzheimer's disease. N Engl J Med. 2010; 362: 329-344.
4. Movement Asl. 2015. Researching Alzheimer's Medicines Setbacks and Stepping Stones Summer 2015. PhMRA.
5. Morrison JH, Hof PR. Selective vulnerability of corticocortical and hippocampal circuits in aging and Alzheimer's disease. Prog Brain Res. 2002; 136: 467-486.
6. Bartzokis G. Age-related myelin breakdown: a developmental model of cognitive decline and Alzheimer's disease. Neurobiol Aging. 2004; 25: 5-18.
7. Smith KDB, kallhoff V, Zheng H, Pautler RG. In vivo axonal transport rate decreases in a mouse model of Alzheimer's disease. Neuroimage. 2007; 35(4): 1401-1408.

8. Stokin GB, Lillo C, Falzone TL, Brusch RG, Rockenstein E, Mount SL, Raman R, Davies P, Masliah E, Williams DS, Goldstein LS. Axonopathy and transport deficits early in the pathogenesis of Alzheimer's disease. Science. 2005; 307(5713): 1282-1288.
9. Zhang L, Lu W, Chen L, Qiu X, Li C, Huang CX, Gong X, Min QC, Lu F, Wan JY, Chao FL, Tang Y. The early changes in behavior and the myelinated fibers of the white matter in the Tg2576 transgenic mouse model of Alzheimer's disease. Neurosci Lett. 2013; 555: 112-117.
10. Lu W, Yang S, Zhang L, Chen L, Chao FL, Luo YM, Xiao Q, Gu HW, Jiang R, Tang Y. Decreased myelinated fibers in the hippocampal dentate gyrus of the Tg2576 mouse model of Alzheimer's disease. Curr Alzheimer Res. 2016; 13(9): 1040-1047.
11. Lee Y, Morrison BM, Li Y, Lengacher S, Farah MH, Hoffman PN, Liu Y, Tsingalia A, Jin L, Zhang PW, Pellerin L, Magistretti PJ, Rothstein JD. Oligodendroglia metabolically support axons and contribute to neurodegeneration. Nature. 2012; 487(7408): 443-448.
12. Baumann N, Pham-Dinh D. Biology of oligodendrocyte and myelin in the mammalian central nervous system. Physiol Rev. 2001; 81: 871–927.
13. Petito CK, Olarte JP, Roberts B, Nowak TS Jr, Pulsinelli WA. Selective glial vulnerability following transient global ischemia in rat brain. J Neuropathol Exp Neurol. 1998; 57(3): 231-238.
14. Xu J, Chen S, Ahmed SH, Chen H, Ku G, Goldberg MP, Hsu CY. Amyloid-beta peptides are cytotoxic to oligodendrocytes. J Neurosci. 2001; 21(1): RC118.
15. Destrooper B, Karran E. The Cellular Phase of Alzheimer’s Disease. Cell. 2016; 164(4): 603-615.
16. Roth AD, Ramírez G, Alarcón R, Von Bernhardi R. Oligodendrocytes damage in Alzheimer’s disease: beta amyloid toxicity and inflammation. Biol Res. 2005; 38: 381–387.
17. Wu Y, Ma Y, Liu Z, et al. Alterations of myelin morphology and oligodendrocyte development in early stage of Alzheimer's disease mouse model. Neuroscience Letters. 2017; 642: 102-106.
18. Desai MK, Mastrangelo MA, Ryan DA, Sudol KL, Narrow WC, Bowers WJ. Early oligodendrocyte/myelin pathology in Alzheimer's disease mice constitutes a novel therapeutic target. Am J Pathol. 2010;177(3): 1422-1435.
19. Schmued L C, Raymick J, Paule M G, Dumas M, Sarkar S. Characterization of myelin pathology in the hippocampal complex of a transgenic mouse model of Alzheimer's disease. Current Alzheimer Research. 2013; 10(1): 30-37.
20. Chao FL, Zhang L, Zhang Y, Zhou CN, Jiang L, Xiao Q, Luo YM, Lv FL, He Q, Tang Y. Running exercise protects against myelin breakdown in the absence of neurogenesis in the hippocampus of AD mice. Brain research. 2018; 1684: 50~59.
21. Desai MK, Sudol KL, Janelsins MC, Mastrangelo MA, Frazer ME, Bowers WJ. Triple-transgenic Alzheimer's disease mice exhibit region-specific abnormalities in brain myelination patterns prior to appearance of amyloid and tau pathology. Glia. 2009; 57(1): 54-65.
22. Wu D, Tang X, Gu LH, Li XL, Qi XY, Bai F, Chen XC, Wang JZ, Ren QG, Zhang ZJ. LINGO-1 antibody ameliorates myelin impairment and spatial memory deficits in the early stage of 5XFAD mice. CNS Neurosci Ther. 2018; 24(5):381-393.

23. Crous-Bou M, Minguillón C, Gramunt N, Molinuevo JL. Alzheimer's disease prevention: from risk factors to early intervention. Alzheimers Research & Therapy. 2017; 9(1): 71.
24. Eric McDade & Randall J. Bateman. Stop Alzheimer's before it starts. Nature. 2017; 547(7662): 153-155.
25. Aboukhatwa M, Dosanjh L, Luo Y. Antidepressants are a rational complementary therapy for the treatment of Alzheimer's disease. Molecular neurodegeneration. 2010; 5: 10.
26. Rozzini L, Chilovi B V, Conti M, Bertoletti E, Zanetti M, Trabucchi M, Padovani A. Efficacy of SSRIs on cognition of Alzheimer's disease patients treated with cholinesterase inhibitors. International Psychogeriatrics. 2010; 22(1): 114.
27. Kim HJ, Kim W, Kong SY. Antidepressants for neuro-regeneration: from depression to Alzheimer's disease. Arch Pharm Res. 2013; 36: 1279e1290.
28. Ivkovic M, Damjanovic A, Jasovic-Gasic M, Paunovic VR. The effects of fluoxetine on cognitive functions in animal model of Alzheimer's disease. Psychiatr Danub. 2004; 16: 15e20.
29. Jin L, Gao LF, Sun DS, Wu H, Wang Q, Ke D, Lei H, Wang JZ, Liu GP. Long-term ameliorative effects of the antidepressant fluoxetine exposure on cognitive deficits in 3TgAD mice. Mol Neurobiol. 2017; 54: 4160e4171.
30. Mowla A, Mosavinasab M, Pani A. Does fluoxetine have any effect on the cognition of patients with mild cognitive impairment? A double-blind, placebo-controlled, clinical trial. J Clin Psychopharmacol. 2007;27(1):67-70.
31. Mowla A, Mosavinasab M, Haghshenas H, Borhani Haghighi A. Does serotonin augmentation have any effect on cognition and activities of daily living in Alzheimer's dementia? A double-blind, placebo-controlled clinical trial. J Clin Psychopharmacol. 2007; 27: 484–487.
32. Dringenberg HC, Diavolitsis P. Electroencephalographic activation by fluoxetine in rats: role of 5-HT 1A, receptors and enhancement of concurrent acetylcholinesterase inhibitor treatment. Neuropharmacology. 2002; 42(2): 154.
33. Perez-Caballero L, Torres-Sanchez S, Bravo L, Mico JA, Berrocoso E. Fluoxetine: a case history of its discovery and preclinical development. Expert Opin Drug Discov. 2014; 9(5): 567-578.
34. Azmitia EC, Gannon PJ, Kheck NM, Whitaker-Azmitia PM. Cellular localization of the 5-HT1A receptor in primate brain neurons and glial cells. Neuropsychopharmacology. 1996; 14(1): 35-46.
35. Li X, Rosborough KM, Friedman AB, Zhu W, Roth KA. Regulation of mouse brain glycogen synthase kinase-3 by atypical antipsychotics. Int J Neuropsychopharmacol. 2007;10(1):7-19.
36. Haroutunian V, Katsel P, Roussos P, Davis KL, Altshuler LL, Bartzokis G. Myelination, oligodendrocytes, and serious mental illness. Glia. 2014; 62(11): 1856-1877.
37. Azim K, Butt AM. GSK3β negatively regulates oligodendrocyte differentiation and myelination in vivo. Glia. 2011; 59(4): 540-553.
38. Lee JY, Kang SR, Yune TY. Fluoxetine prevents oligodendrocyte cell death by inhibiting microglia activation after spinal cord injury. J Neurotrauma. 2015; 32: 633–644.

39. Prut L, Belzung C. The open field as a paradigm to measure the effects of drugs on anxiety-like behaviors: a review. Eur J Pharmacol. 2003; 463(1–3): 3–33.
40. Morris R. Developments of a water-maze procedure for studying spatial learning in the rat. J Neurosci Methods. 1984; 11: 47-60.
41. Chen G, Chen KS, Knox J, Inglis J, Bernard A, Martin SJ, Justice A, McConlogue L, Games D, Freedman SB, Morris RG. A learning deficit related to age and beta-amyloid plaques in a mouse model of Alzheimer's disease. Nature. 2000; 408: 975-979.
42. Gundersen HJ, Bendtsen TF, Korbo L, Marcussen N, Møller A, Nielsen K, Nyengaard JR, Pakkenberg B, Sørensen FB. Some new, simple and efficient stereological methods and their use in pathological research and diagnosis. APMIS. 1988; 96: 379-394.
43. Gundersen HJ, Jensen EB, Kiêu K, Nielsen J. The efficiency of systematic sampling in stereology–reconsidered. J Microsc. 1999; 193(Pt 3): 199-211.
44. Marcussen AB, Flagstad P, Kristjansen PE, Johansen FF, Englund U. Increase in neurogenesis and behavioural benefit after chronic fluoxetine treatment in Wistar rats. Acta Neurol Scand. 2008; 117: 94–100.
45. Bartels C, Wagner M, Wolfsgruber S, Ehrenreich H, Schneider A; Alzheimer's Disease Neuroimaging Initiative. Impact of SSRI therapy on risk of conversion from mild cognitive impairment to Alzheimer's dementia in individuals with previous depression. Am J Psychiatry. 2018; 175(3): 232-241.
46. Behrendt G, Baer K, Buffo A, Curtis MA, Faull RL, Rees MI, Götz M, Dimou L. Dynamic changes in myelin aberrations and oligodendrocyte generation in chronic amyloidosis in mice and men. Glia. 2013; 61(2): 273-286.
47. Sjöbeck M, Haglund M, Englund E. Decreasing myelin density reflected increasing white matter pathology in Alzheimer's disease--a neuropathological study. Int J Geriatr Psychiatry. 2005; 20(10): 919-926.
48. Li H, de Faria JP, Andrew P, Nitarska J, Richardson WD. Phosphorylation regulates OLIG2 cofactor choice and the motor neuron-oligodendrocyte fate switch. Neuron. 2011; 69: 918–929
49. Lu QR, Sun T, Zhu Z, Ma N, Garcia M, Stiles CD, Rowitch DH. Common developmental requirement for Olig function indicates a motor neuron/oligodendrocyte connection. Cell. 2002; 109: 75–86.
50. Sprinkle TJ. 2',3'-cyclic nucleotide 3'-phosphodiesterase, an oligodendrocyte-Schwann cell and myelin-associated enzyme of the nervous system. Crit Rev Neurobiol. 1989; 4(3):235-301.
51. Vogel US, Thompson RJ. Molecular structure, localization, and possible functions of the myelin-associated enzyme 2',3'-cyclic nucleotide 3'-phosphodiesterase.. Journal of Neurochemistry. 1988; 50(6):1667-77.
52. Ubhi K, Inglis C, Mante M, Patrick C, Adame A, Spencer B, Rockenstein E, May V, Winkler J, Masliah E. Fluoxetine ameliorates behavioral and neuropathological deficits in a transgenic model mouse of α-synucleinopathy. Experimental Neurology. 2012; 234(2): 405-416.
53. Dawson MR, Polito A, Levine JM, Reynolds R. NG2-expressing glial progenitor cells: an abundant and widespread population of cycling cells in the adult rat CNS. Mol Cell Neurosci. 2003; 24(2):476-488.

54. Stolt C, Rehberg S, Ader M, Lommes P, Riethmacher D, Schachner M, Bartsch U, Wegner M. Terminal differentiation of myelin-forming oligodendrocytes depends on the transcription factor Sox10. Genes Dev. 2002; 16(2):165-170.
55. Kamphuis W, Orre M, Kooijman L, Dahmen M, Hol EM. Differential cell proliferation in the cortex of the APPswePS1dE9 Alzheimer's disease mouse model. Glia. 2012; 60(4): 615-629.
56. Ciao J, Wang J, Wang H, Zhang Y, Zhu S, Adilijiang A, Guo H, Zhang R, Guo W, Luo G, Qiu Y, Xu H, Kong J, Huang Q, Li XM. Regulation of astrocyte pathology by fluoxetine prevents the deterioration of Alzheimer phenotypes in an APP/PS1 mouse model. Glia. 2015; 64(2):240.
57. Wang J, Zhang Y, Xu H, Zhu S, Wang H, He J, Zhang H, Guo H, Kong J, Huang Q, Li XM. Fluoxetine improves behavioral performance by suppressing the production of soluble b-amyloid in APP/PS1 mice. Curr Alzheimer Res. 2014; 11: 672–680.
58. Zhang P, Kishimoto Y, Grammatikakis I, Gottimukkala K, Cutler RG, Zhang S, Abdelmohsen K, Bohr VA, Misra Sen J, Gorospe M, Mattson MP. Senolytic therapy alleviates Aβ-associated oligodendrocyte progenitor cell senescence and cognitive deficits in an Alzheimer's disease model. Nat Neurosci. 2019; 22(5):719-728.
59. Mi S, Lee X, Shao Z, Thill G, Ji B, Relton J, Levesque M, Allaire N, Perrin S, Sands B, Crowell T, Cate RL, McCoy JM, Pepinsky RB. LINGO-1 is a component of the Nogo-66 receptor/p75 signaling complex. Nat Neurosci. 2004; 7(3):221-8.
60. Mi S, Pepinsky RB, Cadavid D. Blocking LINGO-1 as a therapy to promote CNS repair: from concept to the clinic. CNS Drugs. 2013; 27(7):493-503.
61. Zhao C, Zawadzka M, Roulois AJ, Bruce CC, Franklin RJ. Promoting remyelination in multiple sclerosis by endogenous adult neural stem/precursor cells: Defining cellular targets. J Neurol Sci. 2008; 265(1-2):12-6.

Table

Table 1. Stereological results of the oligodendrocytes in the hippocampus of transgenic mice

		N(OL)-DG	*N(OL)-CA1*	*N(OL)-CA2-3*	*N(CNPase)-DG*	*N(CNPase)*-CA1	*N(CNPase)*-CA2-3
Tg-NS	Mean ($\times 10^4$)	7.82	10.22	10.47	3.84	4.26	3.45
	SD	0.57	1.59	0.78	0.76	0.83	0.95
	OCV (%)	7.32	15.55	7.49	19.92	19.52	27.63
	OCE (%)	5.21	4.56	4.57	7.02	6.66	7.49
Tg-FLX	Mean ($\times 10^4$)	7.41	8.72	10.32	3.93	4.68	3.84
	SD	0.27	1.95	1.52	0.60	0.91	0.69
	OCV (%)	3.70	22.36	14.73	15.36	19.47	18.01
	OCE (%)	5.43	5.21	5.03	6.83	6.30	6.94
Tg+NS	Mean ($\times 10^4$)	9.88	12.31	13.32	2.27	2.65	2.21
	SD	0.55	1.28	1.24	0.40	0.28	0.49
	OCV (%)	5.65	10.45	9.34	17.98	10.67	22.45
	OCE (%)	4.99	4.43	4.36	9.13	8.40	9.37
	Mean ($\times 10^4$)	8.51	11.08	11.36	3.82	4.50	3.61
Tg+FLX	SD	1.09	1.55	1.69	0.58	0.90	0.85
	OCV (%)	12.86	14.01	14.94	15.19	20.09	23.74
	OCE (%)	5.43	4.18	4.19	7.06	6.56	7.35

* N(OL) is the total number of the Olig2 positive oligodendrocytes in the hippocampus, N(CNPase) is the total number of the CNPase positive oligodendrocytes in the hippocampus. The mean value (Mean), standard deviation (SD), observed coefficient of variation (OCV) and observed coefficient of error (OCE) of each parameter are provided.

Figures

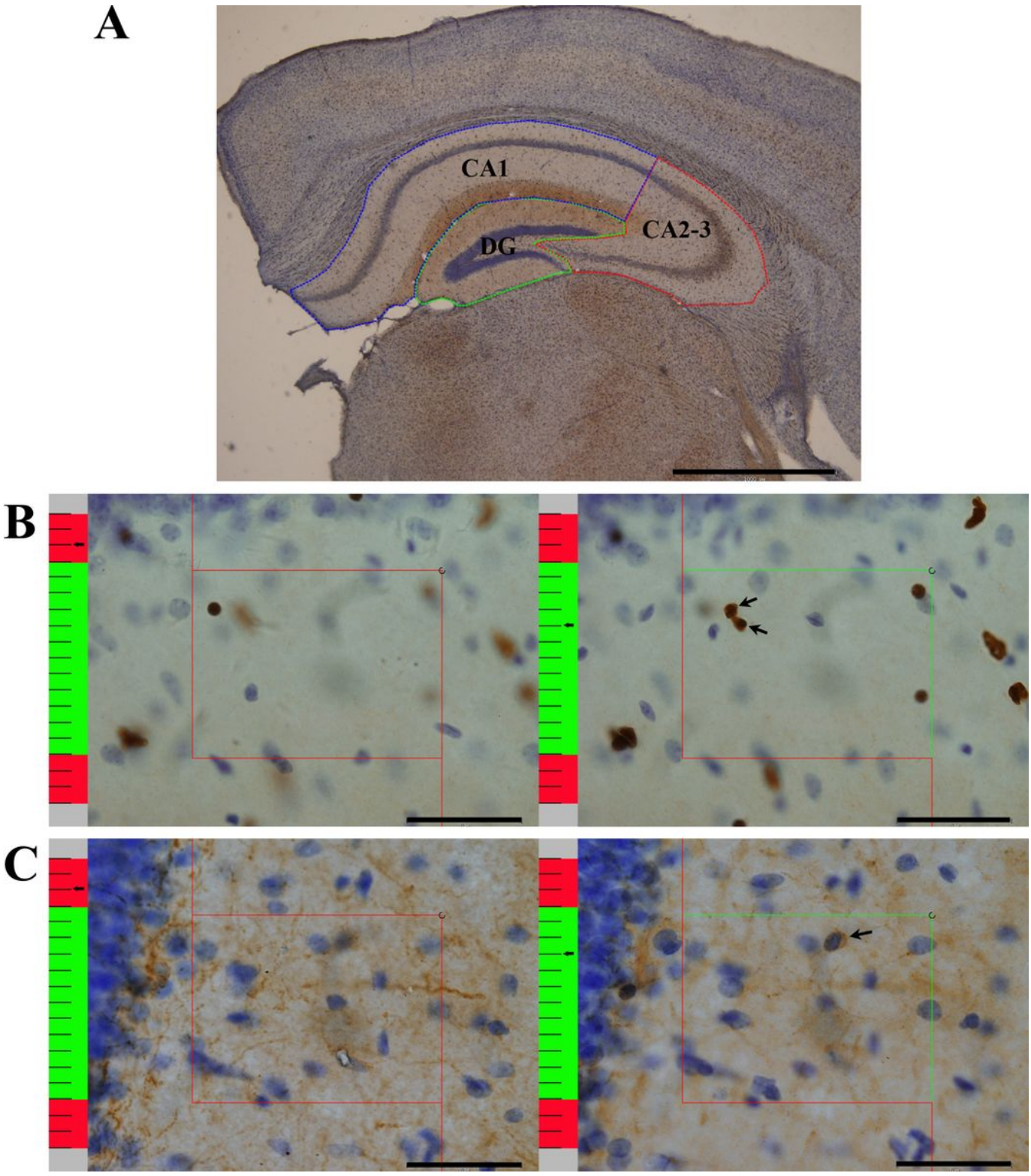

Figure 1

A. After Olig2 immunohistochemistry, the contours of the CA1 (yellow box), CA2-3 (red box) and DG (blue box) regions were traced, and the stereological probe (counting points) was superimposed onto the images using stereology analysis software. Bar = 1000 μm. B. On the left: An illustration of the method used to count the number of Olig2+ oligodendrocytes with the optical disector technique. The nucleus is clearly in focus in the guard zone and is not counted. Bar = 40 μm. On the right: The oligodendrocytes

with nuclei clearly in focus in the counting zone but not in focus in the guard zone are counted. Arrows show the Olig2+ oligodendrocytes that are counted. Bar = 40 μm. C. On the left: An illustration of the method used to count the number of CNPase+ oligodendrocytes with the optical disector technique. The nucleus is clearly in focus in the guard zone and is not counted. Bar = 40 μm. On the right: The oligodendrocytes with their nuclei clearly in focus in the counting zone but not in focus in the guard zone are counted. Arrows show the CNPase+ oligodendrocytes that are counted.

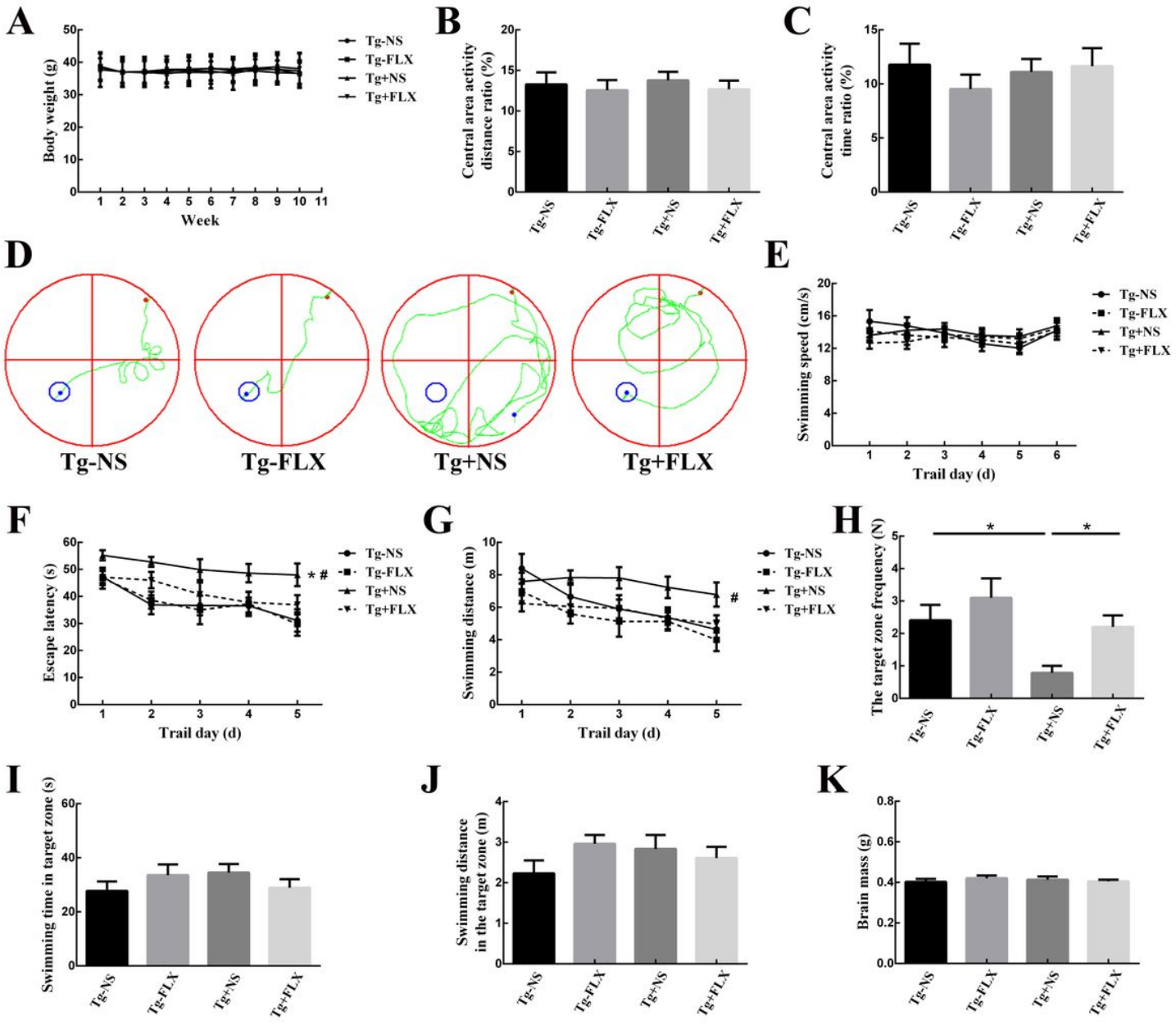

Figure 2

A. Body weight of mice every week (10 weeks) (mean (x) ± SD). B. Central area activity distance ratio (x ± SEM). C. Central area activity time ratio (x ± standard error of the mean (SEM)). D. Tracked locations of the mice in the hidden platform test. The Roman numerals (I, II, III, and IV) represent the first, second, third, and fourth quadrants of the Morris water maze, respectively. E. Swimming speed of the mice in the Morris

water maze test (x ± SEM). F. Escape latencies in the Morris water maze positioning navigation test. Each point represents the average of the four escape latencies (x ± SEM). The asterisk (*) indicates $p < 0.05$ for the comparison of the escape latency of the Tg-NS group and that of the Tg+NS group in the Morris water maze positioning navigation test. The pound sign (#) indicates $p < 0.05$ for the comparison of the escape latency of the Tg+NS group and that of the Tg+FLX group in the Morris water maze positioning navigation test. G. Swimming distance in the Morris water maze positioning navigation test. Each point represents the average of the four escape latencies (x ± SEM). The pound sign (#) indicates $p < 0.05$ for the comparison of the escape latency of the Tg+NS group compared with that of the Tg+FLX group in the Morris water maze positioning navigation test. H. Target zone frequency in the probe trial tests (x ± SEM). * indicates $p < 0.05$. I. Swimming time in the target zone in the probe trial tests (x ± SEM). J. Swimming distance in the target zone in the probe trial tests (x ± SEM). K. Brain mass (x ± SD).

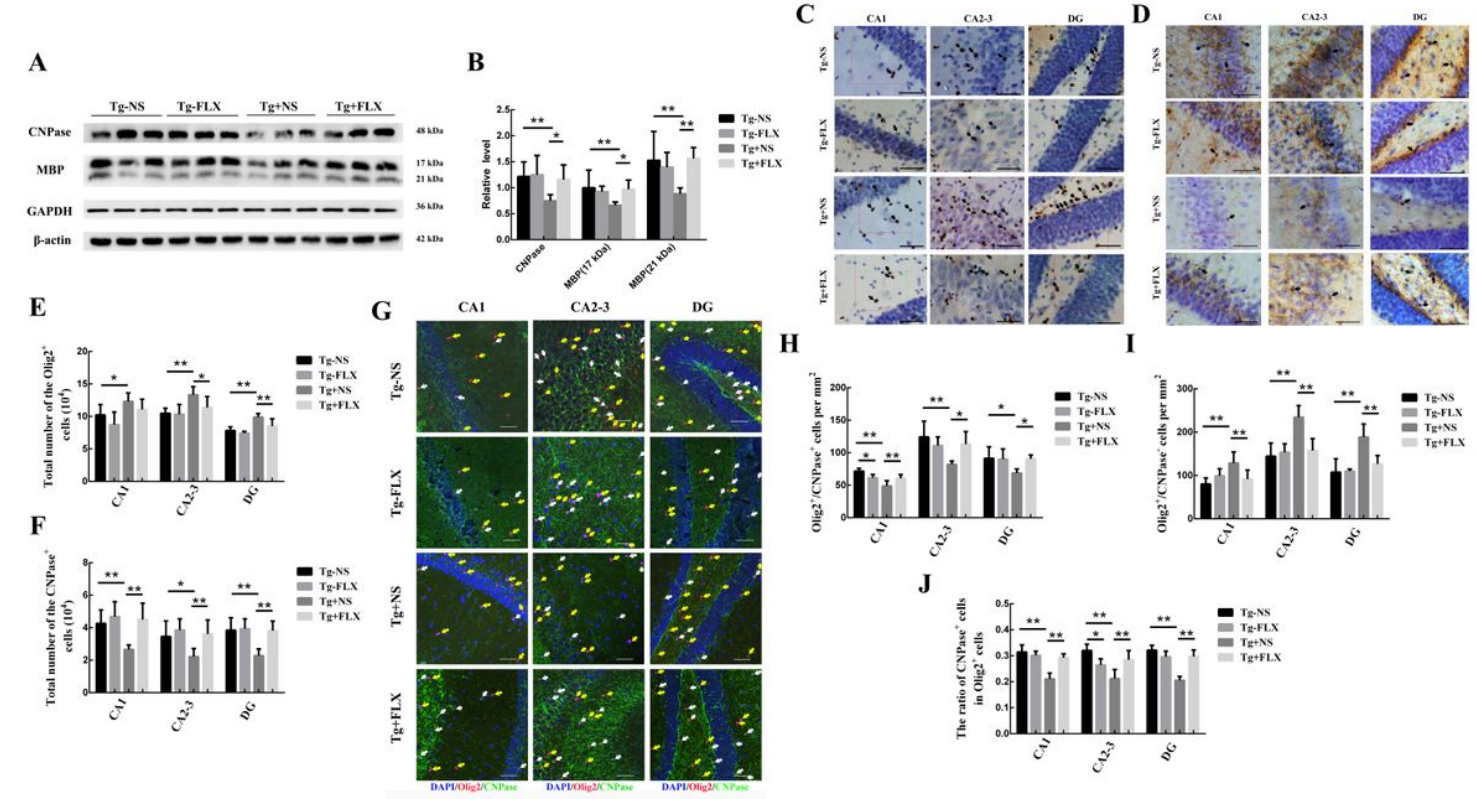

Figure 3

A. Western blot images of CNPase and MBP in the mouse hippocampus. B. The relative protein levels of CNPase and MBP in the hippocampus (x ± SD). * indicates $p < 0.05$. ** indicates $p < 0.01$. C. Oligodendrocyte lineage cells (Olig2+ cells) in the hippocampus. The arrows (→) indicate Olig2+ cells. Bar = 40 μm. D. Mature oligodendrocytes (CNPase+ cells) in the hippocampus. The arrows (→) indicate the CNPase+ cells. Bar = 40 μm. E. Total number of oligodendrocyte lineage cells (Olig2+ cells) in the hippocampus (x ± SD). * indicates $p < 0.05$. ** indicates $p < 0.01$. F. Total number of mature oligodendrocytes (CNPase+ cells) in the hippocampus (x ± SD). * indicates $p < 0.05$. ** indicates $p < 0.01$. G. Immature oligodendrocytes (Olig2+/CNPase- cells) and mature oligodendrocytes (Olig2+/CNPase+ cells) in the hippocampus. Yellow arrows (→) indicate Olig2+/CNPase- cells. White arrows (→) indicate

Olig2+/CNPase+ cells. Bar = 50 μm. H. Density of mature oligodendrocytes (Olig2+/CNPase+ cells) in the hippocampus (x ± SD). * indicates p < 0.05. ** indicates p < 0.01. I. Density of immature oligodendrocytes (Olig2+/CNPase- cells) in the hippocampus (x ± SD). * indicates p < 0.05. ** indicates p < 0.01. J. The ratio of mature oligodendrocytes (Olig2+/CNPase+ cells) to oligodendrocyte lineage cells (Olig2+ cells) in the hippocampus of (x ± SD). * indicates p < 0.05. ** indicates p < 0.01.

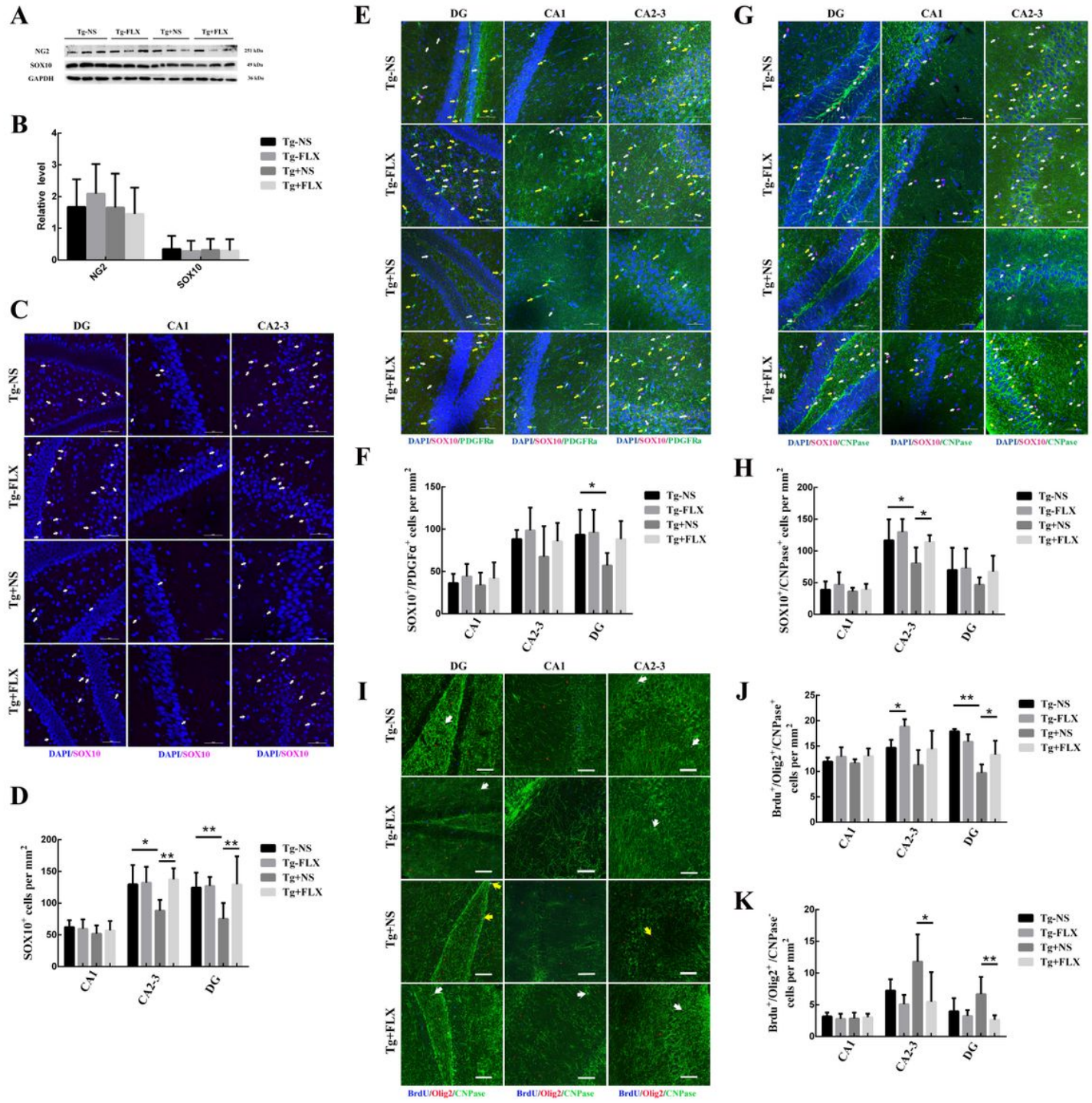

Figure 4

A. Western blot images of NG2 and SOX10 in the mouse hippocampus. B. The relative protein levels of NG2 and SOX10 in the hippocampus (x ± SD). C. SOX10+ cells in the hippocampus. The arrows (→)

indicate the SOX10+ cells. Bar = 50 μm. D. Density of SOX10+ cells in the hippocampus (x ± SD). * indicates p < 0.05. ** indicates p < 0.01. E. SOX10+/PDGFα+ cells in the hippocampus. The arrows (→) indicate SOX10+/PDGFα+ cells. Bar = 50 μm. F. Density of SOX10+/PDGFα+ cells in the hippocampus (x ± SD). * indicates p < 0.05. G. SOX10+/CNPase+ cells in the hippocampus. The arrows (→) indicate SOX10+/CNPase+ cells. Bar = 50 μm. H. Density of SOX10+/CNPase+ cells in the hippocampus (x ± SD). * indicates p < 0.05. I. Newborn immature oligodendrocytes (BrdU+/Olig2+/CNPase- cells) and newborn mature oligodendrocytes (BrdU+/Olig2+/CNPase+ cells) in the hippocampus. Yellow arrows (→) indicate BrdU+/Olig2+/CNPase- cells. White arrows (→) indicate BrdU+/Olig2+/CNPase+ cells. Bar = 50 μm. J. Density of BrdU+/Olig2+/CNPase+ cells in the hippocampus (x ± SD). * indicates p < 0.05. ** indicates p < 0.01. K. Density of BrdU+/Olig2+/CNPase- cells in the hippocampus (x ± SD). * indicates p < 0.05. ** indicates p < 0.01.

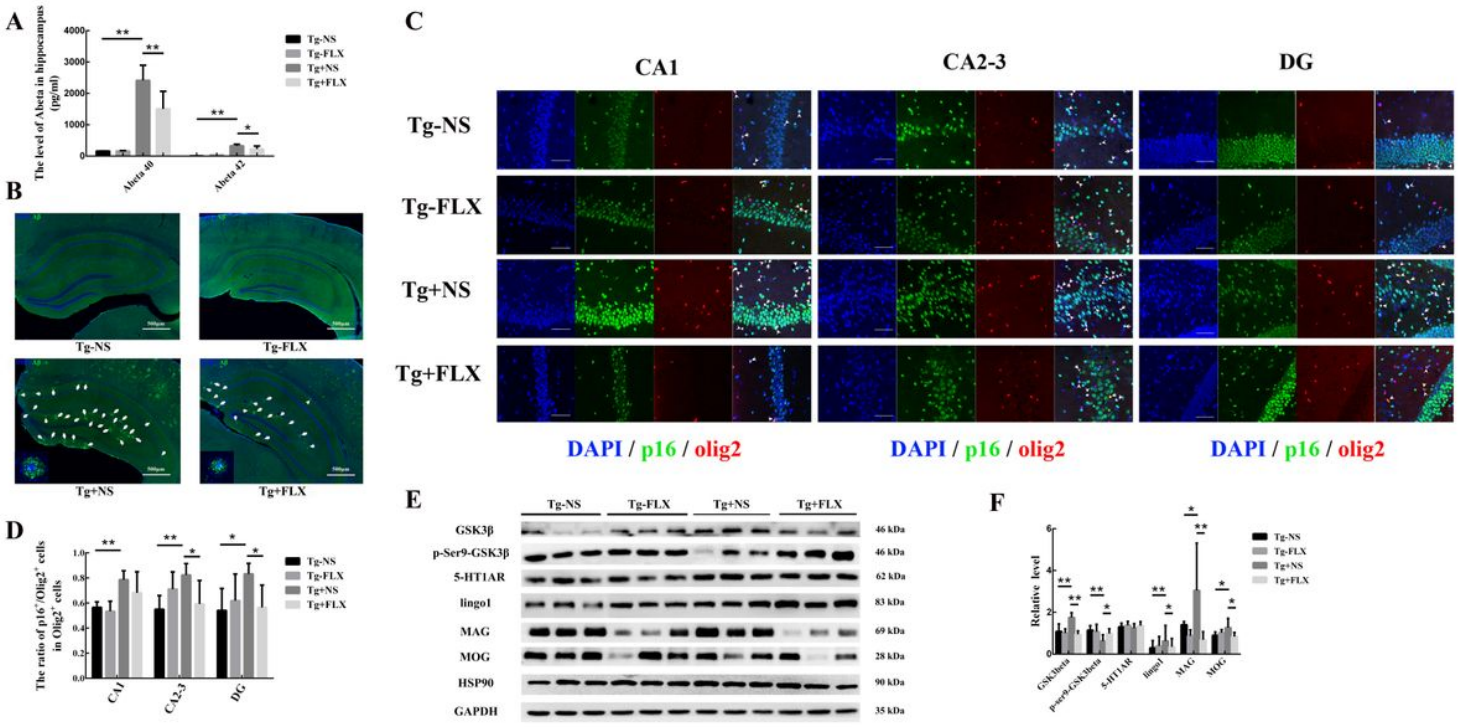

Figure 5

A. ELISA results for soluble human Aβ40 and Aβ42 (x ± SD). * indicates p < 0.05. ** indicates p < 0.01. B. Immunofluorescence-based morphology of Aβ in the hippocampus. Aβ plaques were deposited in the hippocampus of Tg+ mice, and fluoxetine improved Aβ plaque deposition. Arrows (→) indicate Aβ plaques in the hippocampus. Aβ in 10-month-old Tg+NS and Tg+FLX mice is shown at high magnification in each left corner. Bar = 500 μm. C. p16+/Olig2+ cells in the hippocampus. The arrows (→) indicate p16+/Olig2+ cells. Bar = 50 μm. D. Density of p16+/Olig2+ cells in the hippocampus (x ± SD). * indicates p < 0.05. ** indicates p < 0.01. E. Western blot images of GSK3β, p-S9-GSK3β, 5-HT1AR, LINGO1, MAG and MOG in the hippocampus. F. The relative protein levels of GSK3β, p-S9-GSK3β, 5-HT1AR, LINGO1, MAG and MOG in the hippocampus (x ± SD). * indicates p < 0.05. ** indicates p < 0.01.